平　成　１２　年　度

International Meeting on “Best-Estimate” Methods in Nuclear Installation Safety Analysis に関する報告書

平成１３年３月

（財）原子力発電技術機構
原子力安全解析所

本事業は、経済産業省資源エネルギー庁原子力安全・保安院からの委託
〔実用原子力発電施設安全性実証解析（安全性実証解析）〕で実施したものです。

INS/M00-46

平成 13 年 3 月

International Meeting on “Best-Estimate” Methods in Nuclear Installation Safety Analysis

要旨

現在、軽水炉の安全評価に用いる解析手法の詳細化が世界的に進められ、米国では最適評価手法を安全評価に用いることが規制上認められている。また、他の諸外国においても最適評価手法による安全解析の結果をどのように規制上評価すべきか議論が進められている。

米国原子力学会（ANS)、欧州原子力学会（ENS）の主催及び米国産業界（NEI）の共催で開催された“ Best-Estimate” Methods in Nuclear Installation Safety Analysis 国際会議は最適評価手法及び同手法を用いた安全評価等について論議する会議であり、当所における実証解析事業の成果を発表するとともに、実証解析に資する情報を収集した。

当所からは、反応度事故三次元解析コード EUREKA-JINS/S を用いて減速材フィードバック効果を採り入れた解析結果を示し、減速材フィードバック効果が燃料エンタルピ、破損燃料棒本数割合等に及ぼす影響について発表した。

また、当所が冷却材喪失事故（LOCA）解析用に整備を進めている RELAP5/MOD2/INS コードについて、モデル改良、検証状況及びクロスチェック解析コードとして使用する場合の方法等について発表した。

会議では、TRAC、RELAP コードを用いた最適評価手法及びその解析結果についての発表が数多く見られ、発表内容を見ると解析結果の不確かさに基づく安全裕度をどのように考慮すべきか（不確かさ評価）についての発表が多くを占めており、当所においても最適評価手法に加え、その不確かさ評価手法を用いた実証解析を行う必要があると考える。

International Meeting on “Best-Estimate” Methods in Nuclear Installation Safety Analysis

目次

１．序論

現在、軽水炉の安全評価に用いる解析手法の詳細化が世界的に進められ、米国では連邦規制基準 10CFR50.46 と Appndix K において、冷却材喪失事故解析に対して最適評価手法を安全評価に用いることが認められている。また、他の諸外国においても米国の例を参考にして最適評価手法による安全解析の結果をどのように規制上評価すべきか議論が進められている。

米国原子力学会（ANS)、欧州原子力学会（ENS）の主催及び米国産業界（NEI）の共催で開催された“ Best-Estimate” Methods in Nuclear Installation Safety Analysis 会議（以下「BE2000」という。アメリカ-ワシントン DC にて平成 12 年 11 月 12 日～11 月 16 日開催）は最適評価手法及び同手法を用いた安全評価の妥当性等について論議する会議であった。

当所からは以下の 2 件の実証解析事業の成果を発表するとともに、実証解析事業に資する情報を収集した。

(1) Realistic Evaluation of Reactivity Insertion Accidents for a Typical BWR；反応度事故三次元解析コード EUREKA-JINS/S を用いて減速材フィードバック効果を取り入れた解析結果を示し、BWR の減速材フィードバック効果が燃料エンタルピ、破損燃料棒本数割合等に及ぼす影響について発表した。

(2) Status of Modification and Validation of BWR LOCA Audit Analysis Code at NUPEC；当所が冷却材喪失事故（LOCA）解析用に整備を進めている RELAP5/MOD2/INS コードについて、モデル改良、検証状況及びクロスチェック解析コードとして使用する場合の方法等について発表した。

これらの論文を付録に示す。

また、会議では各国の TRAC、RELAP コード等を用いた最適評価手法の整備状況、解析結果及び最適評価コードの規制への適用の現状等に関する情報を収集した。

２．BE2000 会議

２.１ 会議の概要

BE2000 は米国原子力学会（ANS）、欧州原子力学会（ENS）の主催及び米国産業界（NEI）の共催で開催された国際会議「Nuclear Science and Technology :Supporting Sustainable Development Worldwide」の一環として組み込まれた三件のトピカル会議及び一件のワークショップ中の一つであり、米国ではプラントの申請解析やリスク情報による規制（RIR）の成功基準解析等に活用されている最適評価に関して､手法の現状と今後を概観･展望するものである。発表件数は約 84 件で、内訳は米国 34 件、独国 7 件、日本 5 件（NUPEC2 件、東芝 2 件及び原研から 1 件）、その他ロシア(3)、カナダ(3)、イタリア(3)、スイス(3)、ブラジル(2)、韓国(2)、クロアチア(2)、オーストリア(2)、スロベニア(2)、フィンランド(2)、英国(1)、ベルギー(1)、ハンガリー(1)、スロバキア(1)であった。セッションは全体で以下の 10 に分類され、総会を除き 3 セッションが並行して進められた。

(1) 総会
(2) 最適評価手法と許認可・規制要求
(3) 最適評価手法 I、II
(4) 最適評価手法の検証 I～III
(5) 最適手法の燃料及び炉心への応用
(6) BE 評価手法の熱流動解析への応用 I～III
(7) 国際協力プログラムにおける知見及び推奨事項
(8) 最適評価手法支援のためのプラント PIRT（問題定義階層表）手法
(9) 最適解析結果の不確かさ評価 I、II
(10) 最適評価手法とシミュレータ

本会議では、NRC が進めている最適コード統合計画（TRAC、RELAP 等の解析コードを TRAC-M という統合コードにまとめる計画）及び現在 NRC の認可を得ている唯一の最適コードであるウエスチングハウス社（WEC）の WCOBRA/TRAC 更に BWR の過渡・事故解析最適評価コードとして実績の高い TRAC-BF1 等について多数の発表があったため、それらを中心に聴講した。また、当所からは「最適評価手法と許認可・規制要求」及び「最適評価手法の検証」

のセッションでそれぞれ発表を行った。

2.2 各セッションの概要

2.2.1 総会

名誉議長である R.L.Long 氏(LLC)から開会の挨拶があった後、以下の基調講演が行われた。

- E.Wilson 氏(INEEL)は従来の保守性を考慮した決定論的解析手法から、不確かさの評価を含めた最適手法に至るまでの歴史（実験による知見の増大及び解析コードの精度向上）について講演した。
- Wermiel 氏（USNRC；NRR/DSSA の原子炉システム課長）は、規制要求と指針との関係について述べた後、最適評価手法の適用認可は大 LOCA について現在 1 件（WEC の WCOBRA/TRAC）のみであるが、シーメンスや GE も認可申請準備中（S-RELAP、TRACG コード）であること、また、最適手法は RIR（リスク情報による規制）への適用や物理現象の把握に有用で利点があり、NRC は今後その適用を支持すると述べた。
- Glaser 氏(独 GRS)は OECD を中心に進められている（NRC 手法とは異なった）最適評価手法について概説した。欧州では NRC の手法は手順が多く作業量が膨大であるとの批判的見解を持っており、合理化した手法を提案している。しかし、欧州ではまだ規制への具体的な適用実績は無い。
- Tsai 氏(米 Exelon 社)は燃料設計、出力上昇、設計変更、運転・保守等に最適手法は有用であり、産業界としても積極的に活用する意向であると強調した。
- Hockreiter 氏(PSU)は以前 WEC 社で WCOBRA/TRAC の認可作業に従事した経験について述べた。最適評価手法に対する認可上の要求事項は 10CFR50Appendix K のように具体的な記述が無いため準備資料作成に苦労したこと、認可用に最終的に準備した資料は 3 フィートにも上ったこと、コードの検証や適用例の計算のため約 100 個の現象に各々50 ケース程度の計算を実施したため、報告資料は 6 フィートにも上り、多大な時間を要したこと等。

  また、不確かさは現象が進むに連れて増大するとして、一見最適評価手法を否定するかのような見解を示したが、最終的には最適手法は物理現象の理解、保守的マージンの削減などによってプラント運転の合理化等に反映できるメリットが大きく、認可に要した投資は十分に回収可能との見解を示した。

発表後の質疑・応答では不確かさ評価手法、不確かさ評価の 95%信頼度限界などについて質問・討議が行われた。

2.2.2 最適評価手法と許認可・規制要求

本セッションは規制動向及び最適評価手法を許認可の枠組みの一部として確立する上での技術的課題などについてのフォーラムであり、ドイツ、日本、ブラジル、韓国、カナダから発表があった。うち 2 件について以下に記す。

(1) BWR における反応度投入事故の現実的評価（NUPEC）

我が国の原子力安全委員会は燃焼の進んだ燃料の取扱いについて検討し、1998 年に燃焼の進んだ燃料の PCMI 破損しきい値の判断改訂の見直しを行った。このため、特に BWR 炉については反応度投入事故解析における基準に対する安全審査解析結果の裕度は低下しており、反応度事故解析においてより現実的な解析を行うことが求められている。このような状況にかんがみ、高燃焼度燃料の全炉心装荷を想定した代表的な BWR を対象として、反応度投入事故時の燃料挙動を減速材フィードバック効果を取り入れて、反応度事故三次元解析コード EUREKA-JINS/S により詳細に解析し、減速材フィードバック効果が燃料エンタルピ、破損燃料棒本数の割合等に及ぼす影響を評価した結果について発表した。代表的な BWR の RIA 解析における減速材フィードバック効果を三次元解析手法により評価した結果、減速材フィードバック効果は燃料エンタルピ及び破損燃料棒本数に大きく影響することを確認した。中でも、高温破裂による破損割合は 1/10 に減少した。

発表に係る主な質疑応答は以下のとおりである。

Q：燃料エンタルピが最大出力時以降に低下しているのはなぜか？

A：燃料ピンから冷却材への除熱によるものである。

Q：指針改訂前の PCMI 破損しきい値は？、また PWR のしきい値は異なるのか？

A：燃焼度によらず、85 cal/g 一定である。PWR も BWR もしきい値は同じである。

Q：熱水力チャンネルの分割方法は？

A：落下制御棒付近については詳細に、落下制御棒から離れるにつれて数体ごとに 1 チャンネルを割り当てている。

(2) 韓国規制体系での現実的 LOCA 解析手法（韓国 KINS）

韓国では個々の安全審査の安全解析において最適 LOCA コードを用いている。このため KINS では RELAP5/MOD3 を基に LOCA 最適評価コードなどを開発している。これら LOCA 最適評価コードにより Kori1 号炉(PWR)など実機の RTSR(Reload Transient Safety Analysis) などを行っているとのことであった。

2.2.3 最適評価手法 I、II

ここでは NRC が進めている最適コード統合計画 TRAC-M に関連して合計 4 件の発表が行われた。主な内容を以下に示す。

- TRAC-P、B でそれぞれ異なった制御モデルや信号変数の処理を実施しているモジュールを統合し、改善して計算効率を上げる作業を実施中との発表があった。
- 一次元あるいは三次元流動方程式を解く時に発生する疎マトリックスを効率良く解く手法として、SuperLU 疎マトリックス直接解法を開発し計算時間短縮に効果があるとの発表があった。
- TRAC-M を並列化する手法及びループ計算、炉容器内計算、格納容器内計算、三次元核特性計算など要素ごとにプロセッサーを割り当てる方法等を検討したとの発表があった。
- TRAC-M へ TRAC-B の BWR 特有の解析モデルを組み込み、組み込んだコードが従来の TRAC-B と同等の解析機能を有するかどうかの確認解析を実施したとの発表があった。大部分の問題では TRAC-M は TRAC-B と同等の解析が可能との結果を得ているが、実験データとの比較では TRAC-M の方が良好な結果を得ている問題もある。最終的にはより実験に近い結果を出すよう TRAC-M を改良していく方針であるとのことであった。PWR の問題に関しては RELAP5 との相互比較も予定しているとのこと。

  なお、本発表については現行の TRAC-B（TRAC-BF1）が特定の問題（低圧のサブクールボイド）に関しては実験との一致がよくないことが気になった。

2.2.4 最適評価手法の検証 I～III

(1) TRAC-M の検証方法に関して 2 件のシリーズ発表があった。基本は検証用マトリクスを作成し、順次検証していくこということで、その方針及び具体的内容が示された。主な内容を以下に示す。

① TRAC-M は PWR、BWR の過渡・事故すべてを解析対象とするため、検証の範囲は膨大なス

コープとなる。そのため、事象の分類と該当する実験、データの利用可能性などを適切に判断する必要がある。

② 検証マトリクスは以下の 4 分類となる。

- 実験以外の標準データ（OST）との比較（入力エラーチェック、外乱から平衡状態への回帰問題、対称問題、熱伝導等の理論解、数値拡散問題など。）
- 個別実験（SET）との比較
- コンポーネント実験（CET）との比較（CET にはポンプ特性試験、実プラント機能試験などが含まれる。）
- 総合実験（IET）との比較

③ 検証すべき現象は局所レベル（LL：沸騰、凝縮など）、コンポーネントレベル（CL：流量コーストダウン、水位など）及びシステムレベル（SL：自然循環、ループ間の非対称性など）に分類し、その重要度は PIRT（Phenomena Identification and Ranking Table）に従って選定する。PIRT はプラントの種類、プラント型式、発生事象によって異なる。

④ 現状、マトリックスの作成は進捗しており、具体的な問題あるいは実験がマトリックス上に埋められている。また、TRAC の入力デックとして存在しているかどうか、あるいはレポートにデータがあるかどうかも調査・記入されている。

⑤ ただし、大きな課題として気液界面の輸送過程を直接検証する手段がまだ不完全（一部その試みは進んではいるが）であることが述べられている。

(2) BWR LOCA 安全解析コードの整備及び検証状況(NUPEC)

当所で整備した BWR の LOCA 解析コード RELAP5/MOD2/INS のモデル改良、検証状況及びクロスチェック解析コードとして使用する場合の方法等について発表した。同コードは最適評価コードとして十分な機能を有するが、当所では不確かさ評価手法がまだ整備されていないため、当面は保守的な解析条件及び一部のモデルに保守性を加えて使用する方針であることを述べた。それに対して 2 件の質問があった。

Q：検証の過程で高燃焼度 8×8 燃料集合体について沸騰遷移のデータを取っているが、高燃焼度の効果をどうやって取り入れているのか？試験は蒸気・水系か？

A：高燃焼度とは試験集合体のタイプの名称であり、通常の 8×8 試験体とは異なる形状という意味である。燃焼の効果を外挿するという意味ではない。試験は蒸気・水系で行っている。

Q：総合検証結果で被覆管最高温度（PCT）が必ずしも保守的な結果となっていないが、どうやって保守性をも持たせようとしているのか？

A：PCT の応答については気液相間摩擦係数の感度が大きいことを把握しており、現在組み込んでいる相関式の値を小さくすると保守的な結果が得られることを把握している。どの程度保守性を持たせるのが適切か現在検討中である。

(3) WCOBRA/TRAC の検証として 1 件の発表があった。不確かさ評価手法を SPWR に適用することによってブローダウン PCT では平均で 938K、95%限界で 1,073K、リフラッド PCT では平均で 908K、95%限界で 1,046K を得たとのこと。また、重ね合わせの補正効果はそれぞれ 4.4K 及び 4.4K（同じ）であった。

(4) TRAB-3D による BWR 実機の解析（フィンランド VVT）

TRAB-3D は核熱カップリング過渡解析コードであり、三次元 2 群核計算、熱水力並列多チャンネルなど、当所の TRAC-BF1/SKETCH-INS コードと同様なコードである。実際、日本原子力研究所において、TRAB-3D と TRAC-BF1/SKETCH-N 両コードによる冷水注入事象ベンチマーク問題の解析結果の比較などを行った実績もある。

本発表は Olkiluoto 1 号炉で起きたタービンバルブ閉鎖による加圧過渡事象（1985）及び原子炉起動時に発生した炉心振動（1987）を同コードにより解析した結果について紹介している。同コードは CASMO／SIMULATE により定常計算を行い、それらの結果を用いてそれ以後の過渡解析を行う構成となっている。

(5) 三次元動特性解析コード RETRAN-3D による SPERT-Ⅲ解析

同コードの検証を目的に実施した SPERT-Ⅲ実験炉での反応度投入事象の解析結果の紹介。高温低出力時（1MW）と高温高出力時（19MW）の 2 ケースの解析結果が紹介され、高温低出力時については出力時間変化などがよく一致したが、高温高出力時はあまり一致しなかった。このためギャップコンダクタンス、投入反応度などについて感度解析を実施し、一致が悪い原因についてこれらのパラメータの不確かさによるものと結論付けている。

2.2.5 最適手法の燃料及び炉心への応用

(1) 設計ベース、三次元過渡解析による最適手法（アメリカ studvik）

本発表は近代ノード法を用いた動特性炉心解析コード Simulate-3K の概要及び解析結果についての紹介である。Simulate-3K は三次元 2 群拡散コード Simulate-3 を動特性化したものであり、熱水力フィードバックを考慮した過渡解析が可能である。三次元化した現実的解析を行うため核熱計算におけるデータの縮約及び均一化などが不必要である。

同コードでは Ringhals1 号炉の安定性ベンチマーク及び Oskarshamn-3 号炉での不安定事象の解析を行っている。同コードによる Ringhals1 号炉の解析結果を下記に示す。

OECD Ringhals-1 Statistical Summary For Measured v. Predicted Decay Ratio.

	mean error	std dev of error
Cycle 14	-0.028	0.0864
Cycle 15	+0.020	0.0803
Cycle 16	+0.141	0.0560
Cycle 17	+0.116	0.0578

2.2.6 最適評価手法の熱流動解析への応用 I～III

TRAC-BF1 及び TRAC-M(TRAC-B)に関連して 2 件、WCOBRA/TARC 関連で 1 件の発表があった。

- PSU（ペンシルバニア州立大学）の TRAC-BF1 バージョン 98.1 にスイス PSI（ポールシェラー研究所）での修正を加えたバージョンを用いて、被覆管温度が非常に高くなる DBA を超える LBLOCA 及び SBLOCA を解析した結果についての発表があった。今後、RIR における成功基準解析等への適用を考えたためとのことである。このような厳しい条件では TRAC-BF1 は熱伝達係数等の不都合によって計算停止や、ウォーターパッキングなどの振動が起きていたが、本発表ではそれらを回避できる方策と結果が示された。他にも適用に注意を要する幾つかの事項が指摘していた。
- TRAC-M に組み込まれた BWR 関係解析モデルの機能検証のため、TRAC-M と TRAC-B による BWR-6 の SBLOCA の比較解析の発表があった（PSU の発表）。両コードのモデルはピン束部熱伝達や臨界流あるいは相間摩擦等で異なるにもかかわらず、全体として両者の結果（時刻歴など）はよく一致している。ただし、PCT やシステム内冷却材残留インベントリーなどには無視できない違いもあり、その理由及びどちらがより妥当であるかを判断する必要がある。どちらかと言えば、TRAC-M のほうが保守的な計算値を示し、計算も安定している。
- WCOBRA/TRAC の適用例として、PWR、APWR 及び SPWR の LBLOCA を解析した結果を、線出力について整理した発表があった。結果において AP600 に対する LBLOCA の

PCT が PWR でのそれより低いのは線出力が低いためであるが、SPWR では PWR と同等の線出力でもかなり LBLOCA 時の PCT が低い結果となった。この理由は、SPWR ではシステム内冷却材残留インベントリーが設計の特徴から相対的に大きいことによることが分かったとのこと。

2.2.7 国際協力プログラムにおける知見及び推奨事項

ここでは、OECD/NEA あるいは IAEA が主体となって取り組んでいる熱流動最適評価コードのユーザー教育活動が紹介された。当所ではインドネシア・中国に対する研修等を行っており参考になった。

- ユーゴで行われた RELAP、CATHARE、ATHLET の研修プログラムが紹介された。一人前のユーザーを育てるには 2 年間程度のプログラムが必要であり、時々専門家による OJT（2 週間程度）で、スキルの向上を確認している。最終的な目標は与えられた問題に対して適切なノード分割を独力で行える程度のスキルを身に付けさせることである。これらについては、より詳細な資料を入手すれば当所での所内教育や研修に活用できると思われる。
- IAEA では安全解析について基本的な資料をシリーズで発行しているとのことである。これらを入手し、活用すれば当所での所内教育や研修に有効と考えられる。IAEA ではここ 1、2 年でベトナムやインドネシアなどの東南アジアに対して、安全解析のセミナーなどを開催する予定である。

2.2.8 最適評価手法支援のためのプラント PIRT（問題定義階層表）手法

NRC における LBLOCA での PIRT のほか、BWR のドライウェルデブリの輸送問題、AP600 の LBLOCA、WCOBRA/TRAC における適用例、SBLOCA の PIRT などが発表された。すべて米国からの発表であった。

2.2.9 最適解析結果の不確かさ評価 I、II

WCOBRA/TRAC コードの不確かさ評価に関して 2 件の発表があった。

- WCOBRA/TRAC-MOD7A コードは 3、4 ループ PWR 及び 2 ループ UPI(Upper Plenum Injection)PWR に対して NRC から BE LBLOCA コードとして認可されている。最適評価手法は NRC の CSAU 手法に従っている。被覆管最高温度（PCT）の確率分布を得るため、モンテカルロ法を採用した。確率変数は 4 グループ 23 個（初期状態６、出力部分布４、

グローバルモデル 3、局所モデル 10）に分類し、これらの不確かさ幅を設定して WCOBRA/TRAC の計算を行い、PCT の回帰式を得た。回帰式にはモデルの不確かさや計測の不確かさも含めた。

回帰式の確率変数をサンプリングして 10,000 回の計算を行い、PCT の累積分布を求め、それから 95%限界値が求められた。

回帰式は不確かさを線形に重ね合わせているため、WCOBRA/TRAC の実際の計算による PCT と回帰式との差を更に補正する。

- 2 件目の発表では、局所モデルであるホットスポット温度計算モデルとグローバルモデルとの関係を更に分析し、CSAU 手法より計算量の少ない合理的手法を提案している。
- 東芝／東電から TRAC-G による過渡解析の最適評価＋不確かさ評価の結果が発表された。不確かさ評価は CSAU 手法を用い、過渡事象として給水加熱喪失及びタービントリップ事象（バイパス弁閉）が解析された。その結果、前者では申請解析条件で ΔMCPR=0.2 のところが 0.12、後者では申請解析条件で ΔMCPR=0.35 のところが 0.3 となり最適手法の有効性が示された。

２.２.１０ 最適評価手法とシミュレータ

フィンランド（VTT）、米国（SCIENTECH）及びスウェーデン（Studsvik）から APROS、SNAP 及び SIMULATE コードに関する発表があった。

２.２.１１ その他発表

ANS/ENS 本会議で熱流動部門の一部を聴講した。その中で、当所が着手しつつある RIA 時ボイドモデルに関連するサブクール沸騰関連の発表が 4 件有ったため、それらについて紹介する。低圧条件でのサブクール沸騰は研究炉において発生する可能性のある事象として再び注目されているようである。

- スロベニアから三次元解析気泡追跡モデルによる加熱面に沿う方向及び垂直方向のボイド分布・温度分布の解析結果と実験結果が示され、非常によく実験と一致する結果を得たとの発表があった。通常の一次元モデルや二流体モデルでは解析できなかったとのことである。解析は定常状態を対象にしていると思われるが、RIA 時ボイドモデルでは非定常状態でこのような結果が得られることを目指していることから、検討の価値が高い研究である。

- 米国テキサス大 Hassan 教授グループから、定常時サブクールボイドの加熱面に沿う方向の分布について、従来過小評価の傾向のあった RELAP5-3D によるサブクールボイドモデルを Svannah River サブクールボイドモデルに変更することでより実験値に近い結果が得られることを示していた。過渡解析への適用について質問したが、現状では困難とのことであった。
- 上記と同様の問題に対するスロベニアからの発表。解析コードは RELAP5/MOD3.2.2Gamma を使用。遷移流への移行条件を変更、気液界面での凝縮伝熱の係数の変更及び EPRI ドリフトフラックスモデルの Zuber-Findlay モデルへの変更によって、従来過小評価の傾向のあった RELAP5 のボイド分布を非常によく模擬できるようになったとのことである。
- 米国テキサス大 Hassan 教授グループの発表で、RELAP5/MOD3.2 のサブクール沸騰モデルに含まれる壁面熱流束の液相及び沸騰気泡への分配割合に対して種々の提案式を当てはめ、どの式が加熱面に沿う方向のボイド分布をよく示すかを比較していた。結果、Bowring 又は Zeitoun and Shoukri の提案式を使用すると実験とよく一致したとのことである。

３．まとめ

“ Best-Estimate” Methods in Nuclear Installation Safety Analysis では最適評価手法に関する最新の知見及び解析実績を有する各国の専門家が多数出席し、最適評価手法を用いた安全評価について幅広い分野の討論を行った。

当所からは BWR におけるボイドフィードバックを考慮した反応度投入事故の現実的評価結果及び BWR LOCA 解析コードのモデル改良、検証状況等について発表するとともに、各国の最適評価手法の現状及び実機への適用について調査した。

今回の会議の総括を以下に示す。

- 本会議は米国での開催ということで TRAC-M 及び WCOBRA/TRAC に関する多くの発表があり、これらのコードの現状を把握することができた。
- TRAC-M は BWR 版と PWR 版のコード統合によるメリットを強調できる段階にはなく、開発段階のように思われた。BWR を例にとると、その結果が TRAC-B(TRAC-BF1)と無視できない程度に異なる場合があり、現在 TRAC-BF1 を使用しているユーザーに混乱を与えないかという懸念を持った。今後、統一的な見解が望まれる。
- WCOBRA/TRAC については、NRC の認可を受けており、最適評価コードとして認知されたとの印象を受けた。今回の発表は、ほとんどが不確かさ評価に関するものであった。
- 国内メーカーからは TRAC-G による過渡解析を不確かさ評価を含めて実施した発表があり、限界出力比に関する安全余裕の削減に有効との見解を示した。我が国の規制機関においても最適評価コード及び不確かさ評価について、指針の改訂を念頭においた作業を開始すべき時期と考える。

今回の会議では当所の成果を公表するとととともに、専門家よる貴重な意見を得ることができた。また、その他発表聴講を通して世界的な安全解析コード及び手法に関する情報を入手することができた。

これらの成果を当所における実証解析に役立てることとする。

付録

International Meeting on "Best-Estimate" Methods in Nuclear Installation Safety Analysis (BE-2000)
Washington, DC, November, 2000.

Realistic Evaluation of Reactivity Insertion Accidents for a Typical BWR

Hiroshi Yamada, Tetsuo Nakajima, Itiro Komatsu
Nuclear Power Engineering Corporation (NUPEC)
Fujita kanko toranomon bldg., 7F
17-1, 3-chome tranomon,
minato-ku, tokyo 105-0001, JAPAN
(H-YAMADA@nupec.or.jp, NAKAJIMA@nupec.or.jp, KOMATSU@nupec.or.jp)

Keywords: RIA, BWR, EUREKA-JINS/S, void reactivity

ABSTRACT

The three dimensional analysis of RIA for a typical BWR with high burnup fuel were performed using the EUREKA-JINS/S code to understand the realistic fuel behavior during the transient. The fraction of fuel failure was evaluated applying the newly revised failure threshold. For the analysis of RIA in BWR, the influence of void reactivity feedback was studied to understand how it affects on the fuel behavior under the RIA.

The results for a typical BWR indicated that the void reactivity feedback significantly influences to decrease the maximum fuel enthalpy and the fraction of fuel failure.

This paper presents the results of three-dimensional analysis of RIA for a typical BWR

This study was performed under the sponsorship of the Ministry of International Trade and Industry (MITI)

1. INTRODUCTION

The results of recent reactivity insertion accident (RIA) experiments with high burnup fuel performed in France (CABRI; Schmitz, 1994) and in Japan (NSRR; Fuketa, 1995) indicated that some fuel failed at the lower deposited energy in the fuel than was previously assumed.

Taking it seriously, Japanese Nuclear Safety Commission (NSC) had reviewed the current licensing criteria for RIA, and the failure threshold for high burnup fuel was revised based on the new experimental data. The new failure threshold related to PCMI is defined as function of fuel burnup and it decreases stepwise with increasing fuel burnup. This change would directly affect the safety assessment of RIA.

Historically, the point kinetics model or one dimensional kinetics model using core wide coefficients having a significant conservatism has been employed for the safety assessment of RIA. This approach is insufficient to evaluate the distribution of fuel

enthalpy in the core considering the variation of fuel burnup. In order to investigate the influences of fuel burnup and decreased threshold on the safety assessment of RIA, the realistic analysis by using detailed three-dimensional method is necessary.

Three-dimensional neutronic transient code “EUREKA-JINS/S”(NUPEC, 1998) is a modification of EUREKA-SPACE (Inabe, 1977) code which was originally developed in JAERI. The EUREKA-JINS/S code has been modified in detail at NUPEC/INS and it has been used for the audit calculations on the safety analysis of RIA at NUPEC/INS to support the safety examination conducted by MITI (Ministry of International Trade and Industry).

The three dimensional analysis of RIA in typical BWR with high burnup fuel were performed using the EUREKA-JINS/S code to understand the realistic fuel behavior during the transient and to evaluate the safety margin accurately. The fraction of fuel failure was evaluated applying the newly revised failure threshold. For the analysis of RIA in BWR, the void reactivity feedback was considered to understand how it affects on the fuel behavior under the RIA.

The results of three-dimensional analysis of control rod drop accident for a typical BWR considering the void reactivity feedback indicated that the void reactivity feedback significantly influenced to decrease the maximum fuel enthalpy and the fraction of fuel failure.

This paper presents the outline of three-dimensional neutronic transient code “EUREKA-JINS/S”, the results of code verification and calculated results of the RIA in typical BWR with high burnup fuel.

2. Fuel Safety Criteria for RIA

The fuel safety criteria for RIA is defined in “the Evaluation Guide for Reactivity Insertion Events of Light Water Nuclear Power Reactor Facilities” (Nuclear Safety Commission, 1984) in Japan. For the RIA, the limit on the maximum fuel enthalpy is used as fuel safety criteria to avoid the loss of coolable geometry and the generation of coolant pressure pulses. Based on the data from the NSRR RIA experiments, a fuel enthalpy level of 230 cal/g is used as the acceptance limit for the RIA in Japan. This limit must be readjusted considering the decrease of melting point of fuel with increase of burnup and with addition of gadolinium or plutonium.

In Japan, the fuel failure threshold to evaluate the number of fuel rod failure under the RIA is mostly based on the data from the NSRR RIA experiments. The fuel failure mechanism is classified into the following two types.

- Pellet-Cladding Mechanical Interaction (PCMI) Failure
- High-Temperature Rupture

Depending on the fuel failure mechanism, the individual fuel failure threshold is defined respectively. The threshold for the fuel failure due to pellet-cladding mechanical

interaction (PCMI) has been revised in 1998 based on the new data from the CABRI and NSRR RIA experiments. Since the PCMI failure occurs in the early phase of the RIA, the burnup dependent limit for PCMI failure is defined by the initial fuel enthalpy increase as shown in Fig.1. The initial fuel enthalpy increase from the time zero to the time t_e defined in Fig.2 is used to evaluate the PCMI failure.

Test ID	No Failure	Failure	Test ID	No Failure	Failure
PWR	◇	◆	SPERT,PBF	△	▲
BWR	□	-	CABRI(UO_2)	▽	▼
JMTR	○	●	CABRI(MOX)	⊕	+

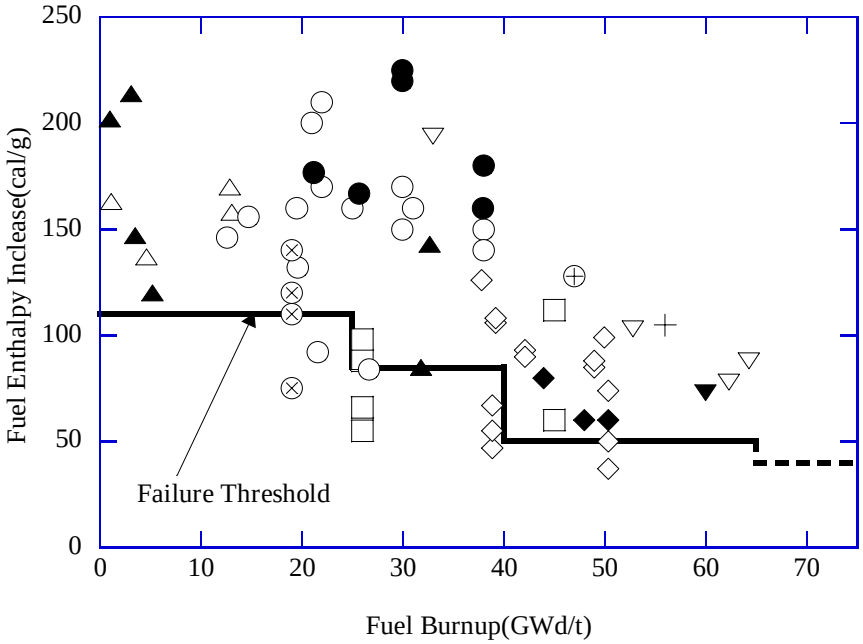

Fig. 1 Fuel failure threshold related to PCMI

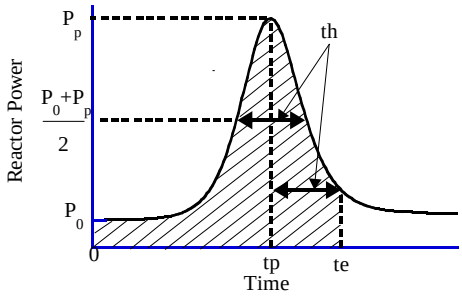

Fig. 2 Definition of the time t_e to calculate the initial fuel enthalpy increase use used for the evaluation of PCMI failure

The high-temperature rupture related to critical heat flux is observed in the fuels that have the pressure difference over 6 kg/cm^{2}g between internal and external pressure

of the fuel. The threshold for the high-temperature rupture is defined by the total fuel enthalpy as a function of pressure difference between internal and external pressure of fuel rod, as shown in Fig.3. The maximum fuel enthalpy in each rod is used to evaluate the high-temperature rupture. The internal and external pressure difference of fuel rod would exceed 6 kg/cm^{2}g in the cold start-up condition (at atmospheric pressure) of BWR, therefore the fuel failure due to high-temperature rupture is evaluated in the RIA analysis of BWR.

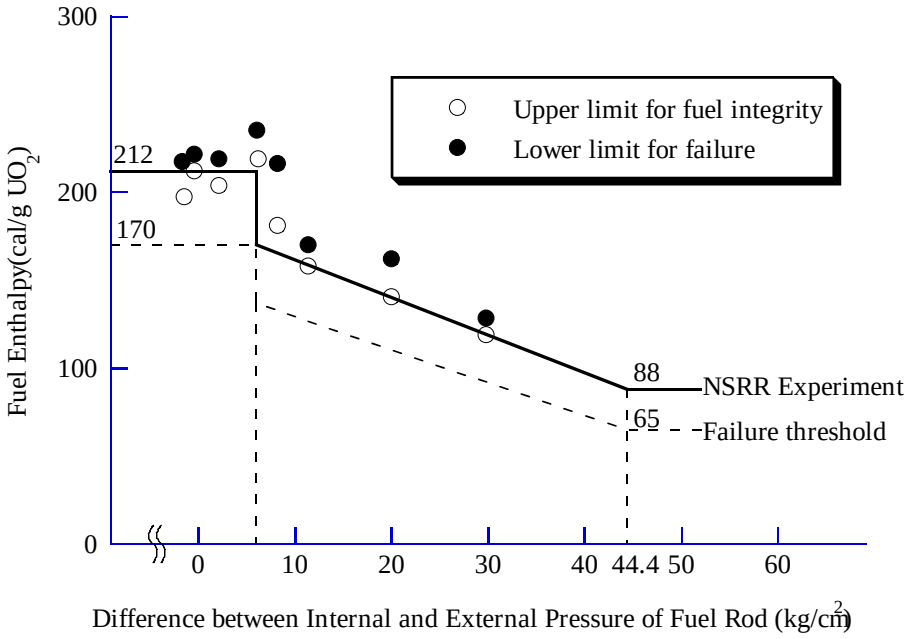

Fig. 3 Failure between threshold defined as function of pressure difference between internal and external pressure of fuel rod

3. Outline of EUREKA-JINS/S Code

Three-dimensional neutronic transient code “EUREKA-JINS/S” is a modification of EUREKA-SPACE code which was originally developed in JAERI.
In the EUREKA-JINS/S code, the model to calculate the reactivity insertion due to control rod movement and the feedback due to changes of fuel temperature and moderator density is completely revised by applying the perturbation theory.

The code uses a quasi-static kinetics model coupled with a multi-channel thermal-hydraulic model based on a homogeneous flow model. In the quasi-static kinetics model, the space-time neutron kinetics is described by assuming variable separation between the amplitude function and the shape function. The amplitude function is described by point kinetics equations for up to six-delayed neutron precursor groups indicating the overall dynamic behavior of core power. The shape function is described by two-group diffusion equations indicating the spatial power distribution in the core. In calculating the shape function, three-dimensional diffusion equations are solved by using CITATION code (Fowler, 1971).

Each function is solved within each sequential time step. The amplitude function is solved at very small time steps, while the shape function is solved at arbitrarily specified time steps when a significant change of reactivity is occurred in it. Within a time step for the shape function, the spatial distribution of the neutron flux is not revised and the change of reactivity used in the amplitude function is obtained based on the perturbation theory. The change of reactivity is obtained by multiplying the weighting function and the change of cross sections and integrating overall the core.

The thermal-hydraulic model in EUREKA-JINS/S is based on 3-balance equations for a homogeneous flow. In the thermal-hydraulic calculation, the core is modeled with multiple parallel coolant channels and each channel is divided into a number of axial nodes. The thermal heat transfer from the fuel to the coolant is calculated by solving the radial one-dimensional heat conduction equation with the Crank-Nicholson method for each axial node of each channel. The pressure drop across the channel is calculated by solving the momentum equation with the Newton-Raphson iterative procedure. In the calculation, the fluid mass in each channel is readjusted to keep the initial pressure drop throughout the transient as a conservative boundary condition. The fluid mass is suppressed in accordance with the increase of void fraction to keep the initial pressure drop in a channel.

In the saturated boiling region, the void fraction is calculated by using the homogeneous flow model in which no slip is assumed between vapor and liquid. In the subcooled boiling region, the Levy model (1967) is used to determine the departure point of boiling and the Zuber-Findlay model (1965) based on drift flux model is used for the void-quality correlation.

For calculating the heat transfer from the fuel to the coolant, the heat transfer correlation models specified in “the Evaluation Guide for Reactivity Insertion Events of Light Water Nuclear Power Reactor Facilities” are used.

4. Verification of EUREKA-JINS/S

To assess the three-dimensional diffusion model incorporated in the EUREKA-JINS/S code, the steady-state core analysis has been performed against the Tihange unit-2 operating data. The Tihange unit-2 is a Framatome type 3-loop PWR, for which the operating data throughout the Cycle 10~12 operations have been obtained from the Tractabell of Belgium. It is pointed out that the eight MOX fuel assemblies were first loaded into the peripheral core in the Cycle 12 operation.

The three-dimensional power distributions have been calculated by EUREKA-JINS/S at EOC of Cycle 12 operation and compared with the measurements. The result of comparison for the axially collapsed two-dimensional power distribution is presented in Fig.4. The differences between the calculations and measurements are shown in Fig.4 for all assemblies in the core. The results of calculations were in good agreement with the measurements, where the RMS error on all assemblies was within 2.2%. The core averaged axial power distribution is compared with the measurement was also in good agreement.

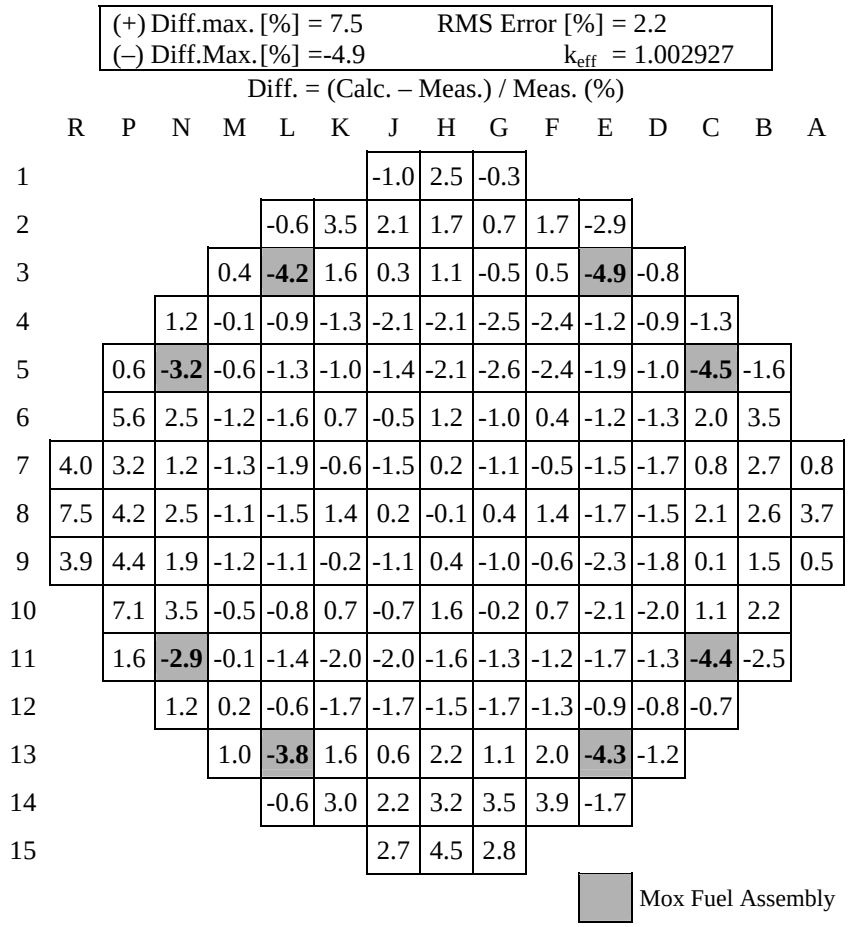

Fig. 4 Comparison of two-dimensional power distribution at EOC

In contrast to the good results of RMS error on two-dimensional power distributions, the larger errors were found to exist for the MOX fuel assemblies compared with the UO_2 fuel assemblies as shown in Fig.4. The measured power distributions are translated from the detector reaction rates. A part of instrument signal is produced from the gamma ray interaction. The fraction of the U-235 fission chamber signal generated by gamma ray is small (<5%), but the fraction is very different for instruments in MOX fuel assemblies versus UO_2 fuel assemblies since the thermal flux and neutron reaction rate are so low in MOX fuel assemblies. Thus if the gamma ray contributions to the detector signals are not accounted for properly in the translation of detector signals to the power, a few percents of under-prediction will be expected in the calculated power for MOX fuel assemblies.

5. Analysis of RIA in BWR

5.1 BWR Core Model

With the support of the utility, full core three-dimensional model of a BWR core was prepared. The BWR core model represents a typical BWR-5 core on a equilibrium cycle. The core models for end of cycle (EOC) and both at cold and hot zero power (CZP

and HZP) were used in the RIA analysis. The core includes 764 type-A fuel assemblies of 9×9 fuel configuration with burnups up to a assembly maximum of 55 GWd/t. The control rod patterns for two conditions of CZP and HZP are shown in Fig. 5 and Fig. 6, respectively. In each core, the dropped rod was located in the periphery of the core. The core model for each condition was modified such that the design-based rod worth of 1.0 %Δk/k was increased to 1.3 %Δk/k. This was achieved by exchanging a few fuel assemblies adjacent to the dropped rod into another positions. The cross sections for each core were provided by the utility and validated against initial steady-state conditions.

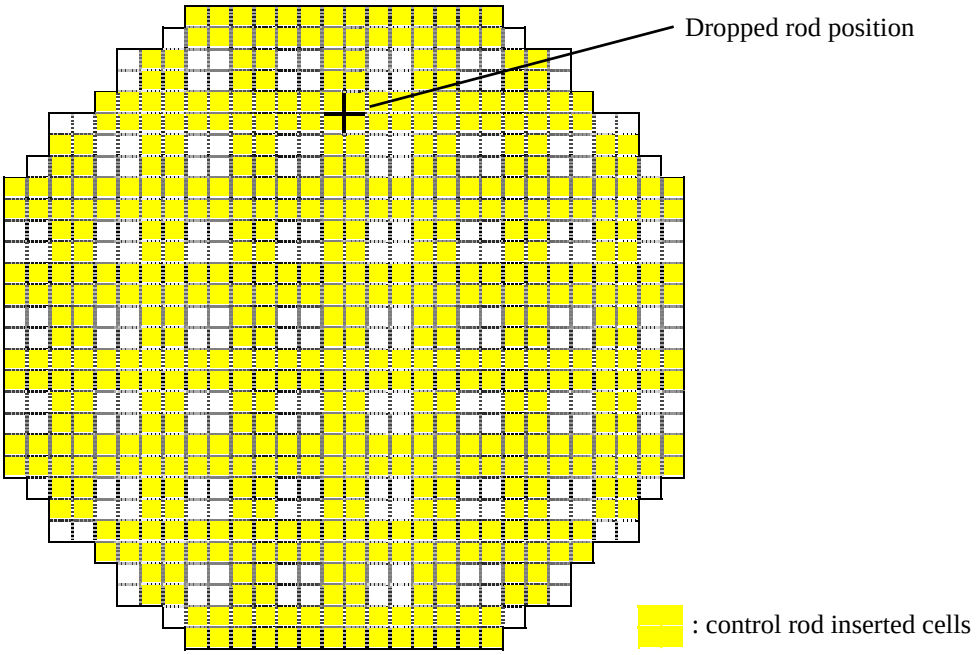

Fig. 5 Initial control rod pattern for EOC and CZP

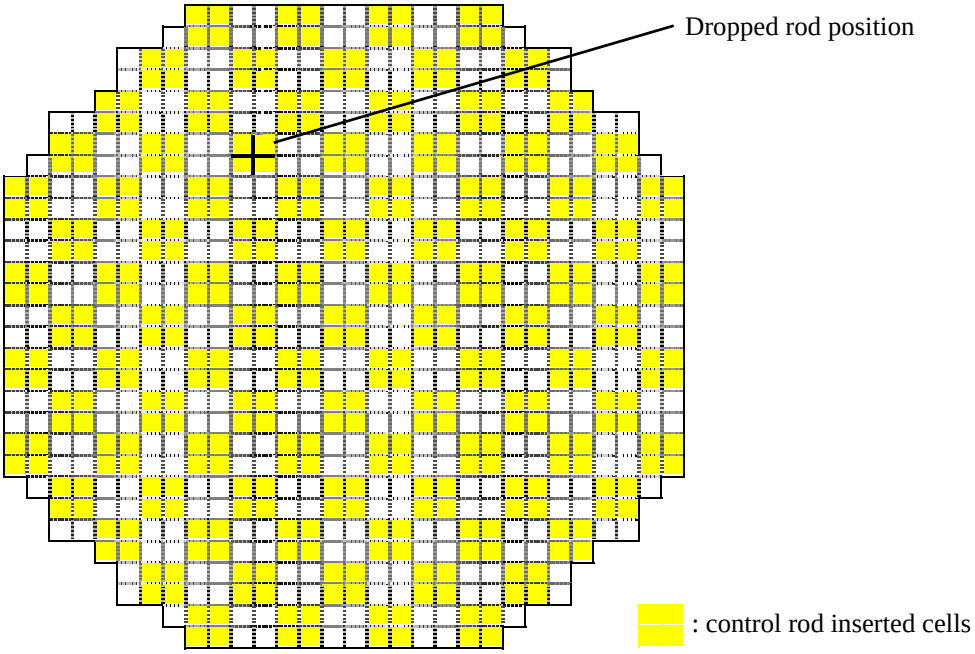

Fig. 6 Initial control rod pattern for EOC and HZP

In the neutronic model, the radial mesh was 4 nodes per assembly and the number of axial planes was 48 in the effective fuel region. In the thermal-hydraulic model, the core region was modeled by 100 thermal-hydraulic channels for CZP case and by 112 channels for HZP case, respectively. In the region around the dropped rod, each channel represented a single assembly in order to accurately reflect the thermal-hydraulic reactivity feedback effects following a control rod drop. In other region, each channel represented several fuel assemblies. The number of axial nodes in each channel is 20.

5.2 Core Conditions and Assumptions

The analysis of control rod drop accident in BWR was performed for two conditions of CZP and HZP at end of cycle (EOC). The initial core conditions and parameters used in the analysis for each case are shown in Table 1. In the analysis, the dropped rod worth was chosen very conservatively to keep the similar assumptions used in the conventional safety analysis.

The void generation causes negative reactivity feedback effect and plays an important role in suppressing the fuel enthalpy increase for a BWR. In the current safety analysis of RIA, the void reactivity feedback is not applied so as to make the results more severe. The current void generation models are based on the experiments under steady-state conditions, therefore, these models are not verified against the prompt heating condition found during a RIA. However, in order to understand the realistic fuel enthalpy increase and safety margin during the transient, the void reactivity feedback calculated by the current models was applied in the analysis of BWR RIA. Furthermore, to understand

how it affects on the fuel behavior under the RIA, another calculations were performed by neglecting the void reactivity feedback.

Table 1 Core Conditions and Parameters for RIA Analysis in BWR at EOC

Core condition/Parameter	Value/Assumption	
	Cold Zero Power(CZP)	Hot Zero Power(HZP)
Initial power level (MW)	3.293×10^{-5} (10^{-8} rated)	3.293×10^{-3} (10^{-6} rated)
Coolant inlet pressure (kg/cm^{2}A)	1.58	72.3
Coolant inlet temperature (°C)	20	286
Coolant flow	20 % of nominal	
Dropped rod worth (%Δk/k)	1.3	
Control rod drop speed (m/s)	0.95	
Delayed neutron fraction (%)	0.58	0.56
Prompt neutron lifetime (μs)	48	41
Void reactivity feedback	Applied and calculated by using the current models	
Ratio of direct moderator heating	0.02	

Following the Japanese evaluation guide for RIA, the fuel enthalpy limit of 230 cal/g was readjusted to 200 cal/g by considering the decrease of melting point of fuel with increase of burnup and with addition of gadolinium. The number of fuel rod failures was evaluated for two failure mechanisms respectively. The number of fuel rod failures due to PCMI was calculated by applying the PCMI failure threshold shown in Fig.1. The number of fuel failures due to high-temperature rupture for this event was calculated by using the burnup dependent failure threshold shown in Fig. 7. The limit of 92 cal/g up to 40 GWd/t was derived from the failure threshold shown in Fig.3 by conservatively assuming the pressure difference of 30 kg/cm^{2}g. The limit of 65 cal/g was conservatively used for the fuels over 40 GWd/t.

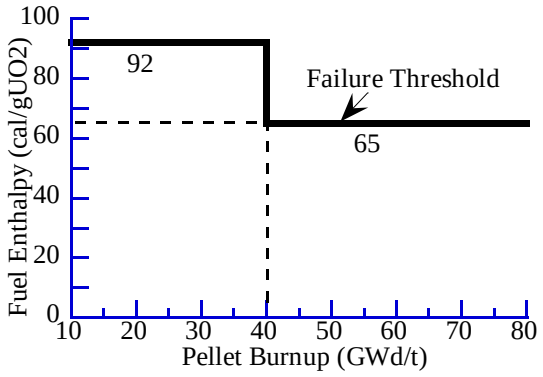

Fig. 7 Burnup dependent failure threshold for high-temperature rupture

5.3 Results for a Core at EOC and CZP

The three-dimensional analysis of control rod drop accident was performed for end of cycle (EOC) and at cold zero power (CZP). Fig. 8 shows the reactor power during the transient on a logarithmic scale relative to nominal power. The figure also shows the differences between the results with and without void reactivity feedback. For both cases, the power pulse started at about 0.9 seconds and reached a maximum value of 4.7 of nominal power at about 1.2 seconds. At that time, the power pulse was terminated due to the negative Doppler reactivity feedback. The power for the case with void reactivity feedback decreases gradually after termination of power pulse, while for the case without the void reactivity feedback, the power rises slowly until the plant is scrammed.

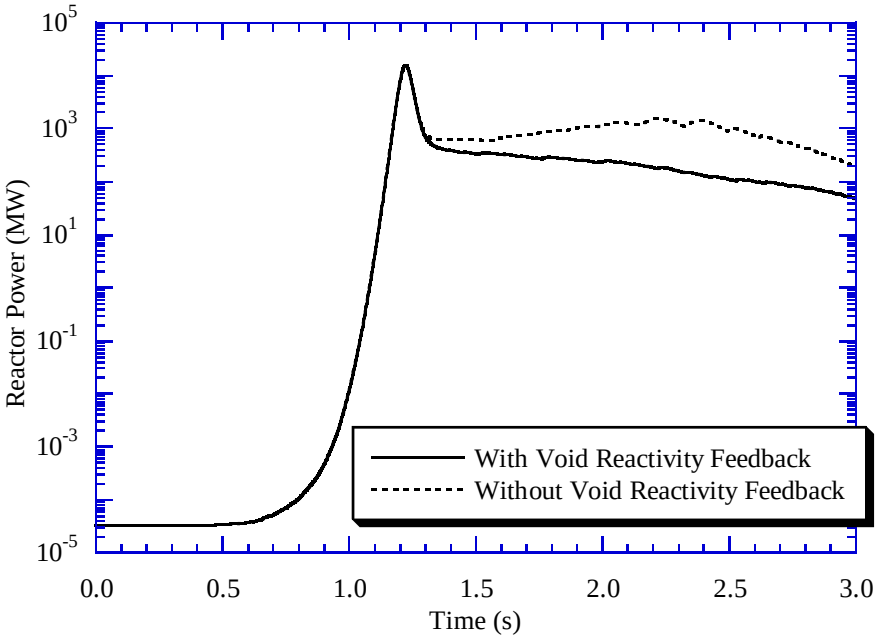

Fig. 8 Reactor power during the transient for EOC and CZP

Fig. 9 shows the trend of the different reactivity feedback components during the transient for the case with void reactivity feedback. The figure also shows the power pulse on a linear scale. This figure shows that the boiling in the core initiated right after the termination of power pulse and the void reactivity feedback acts effectively to reduce the power increase as shown in Fig. 8. In the cold start-up condition, there is about 80 °C coolant subcooling at atmospheric pressure and, therefore, this delayed the onset of void generation caused by the rod drop accident.

Fig. 10 shows the maximum fuel enthalpy during the transient. The figure also shows the differences between the results with and without void reactivity feedback. For the case with void reactivity feedback, the fuel enthalpy increased rapidly due to the power pulse and reached a maximum value of 108 cal/g at about 1.3 seconds. At that time, the heatup due to the power pulse was terminated by the negative Doppler reactivity feedback and also the heatup after power pulse was suppressed by the void reactivity feedback. While in the case without the void reactivity feedback, the fuel enthalpy rises

slowly after termination of power pulse until the plant is scrammed and reaches a maximum value of 135 cal/g at about 2.6 seconds. This result indicates that the void reactivity feedback influences effectively to reduce the peak fuel enthalpy.

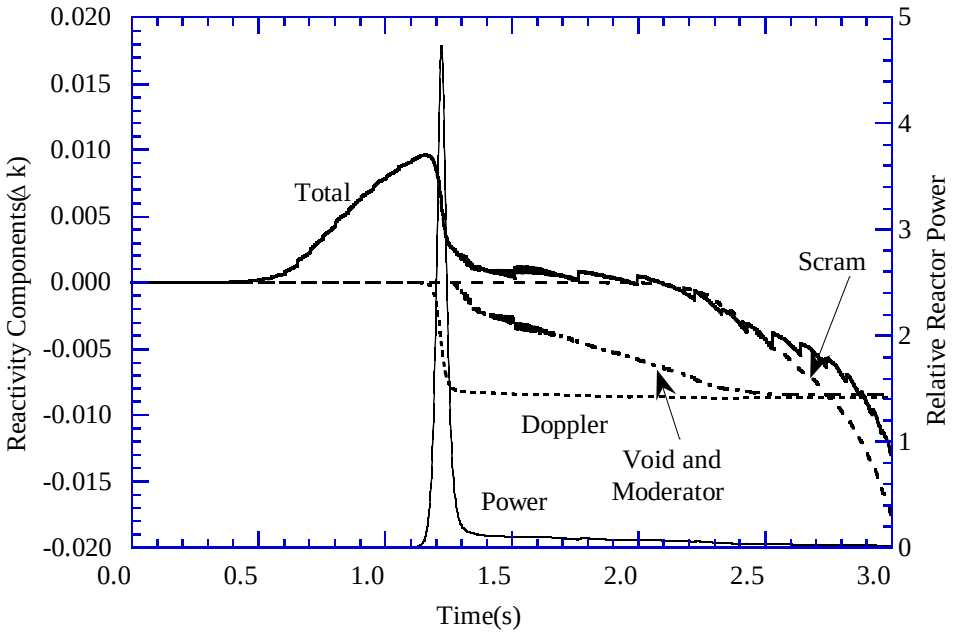

Fig. 9 Reactivity components during the transient for EOC and CZP

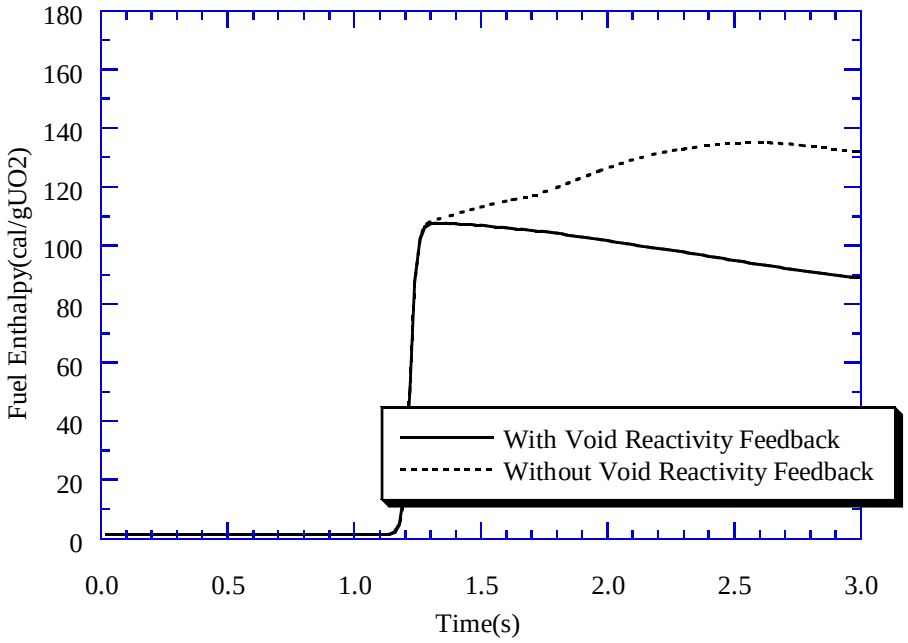

Fig. 10 Maximum fuel enthalpy during the transient for EOC and CZP

Fig. 9 shows the trend of the different reactivity feedback components during the transient for the case with void reactivity feedback. The figure also shows the power pulse on a linear scale. This figure shows that the boiling in the core initiated right after the termination of power pulse and the void reactivity feedback acts effectively to reduce the power increase as shown in Fig. 8. In the cold start-up condition, there is about 80°C coolant subcooling at atmospheric pressure and, therefore, this delayed the onset of void generation caused by the rod drop accident.

Fig. 10 shows the maximum fuel enthalpy during the transient. The figure also shows the differences between the results with and without void reactivity feedback. For the case with void reactivity feedback, the fuel enthalpy increased rapidly due to the power pulse and reached a maximum value of 108 cal/g at about 1.3 seconds. At that time, the heatup due to the power pulse was terminated by the negative Doppler reactivity feedback and also the heatup after power pulse was suppressed by the void reactivity feedback. While in the case without the void reactivity feedback, the fuel enthalpy rises slowly after termination of power pulse until the plant is scrammed and reaches a maximum value of 135 cal/g at about 2.6 seconds. This result indicates that the void reactivity feedback influences effectively to reduce the peak fuel enthalpy.

Fig. 11 shows the maximum fuel enthalpy distributions in the core. The maximum fuel enthalpy occurred in the one cycle burned fuel assembly adjacent to the dropped rod. The result indicates that the maximum fuel enthalpy in an assembly is correlated by the distance of the assembly from the dropped rod position, the control rod pattern and the burnup of the fuel.

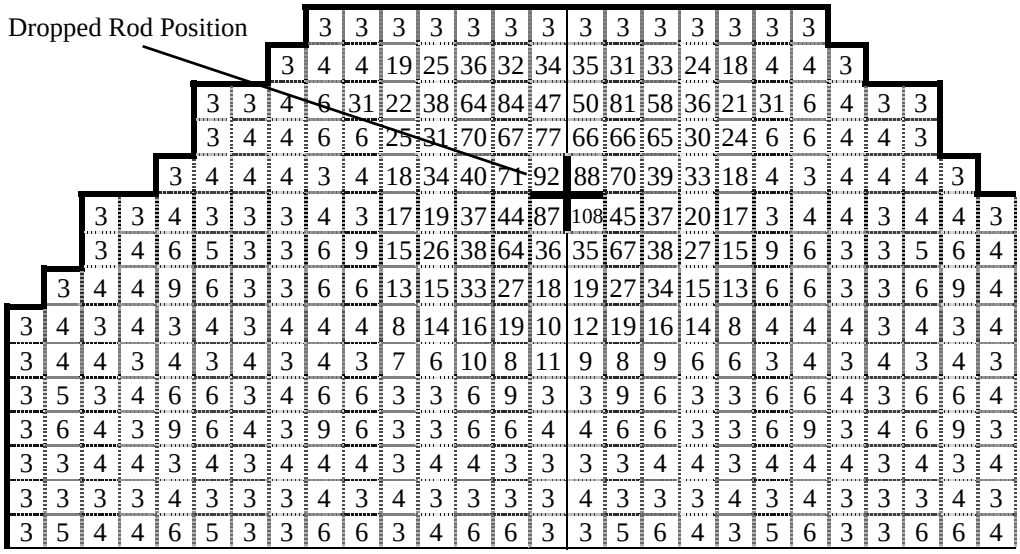

Fig. 11 Distribution of maximum fuel enthalpy of each assembly for EOC and CZP

Table 2 presents the numbers of fuel failures due to PCMI for the control rod drop accident. In Table 2, the difference between the results with and without void reactivity feedback is also compared. Since the initial fuel enthalpy increase at the time t_e defined in Fig.2 for two cases shows small difference, therefore, the difference between two cases for number of fuel failures due to PCMI is small. The void reactivity feedback becomes effective in the later phase of this event due to the delay of void generation at cold start-up condition, therefore the void reactivity feedback shows smaller effect on the initial fuel enthalpy increase and hence on the fuel failures due to PCMI.

Table 2 Summary of the results performed for a BWR at EOC and CZP

Item	Results	
	With Void Reactivity Feedback	Without Void Reactivity Feedback
Maximum reactor power (ratio to nominal)	4.7	4.8
Maximum fuel enthalpy (cal/g)	108	135
Maximum initial fuel enthalpy increase (cal/g)	106	108
Number of fuel failures due to PCMI	110	127
Number of fuel failures due to high-temperature rupture	36	329

In contrast to the small difference for the results of fuel failure due to PCMI between the cases with and without void reactivity feedback, the large difference was obtained for the results of fuel failure due to high-temperature rupture between two cases as shown in Table 2. The maximum fuel enthalpy during the transient for the case without void reactivity feedback is about 26 % higher than the results with void reactivity feedback as shown in Fig. 10. Due to this difference, the number of fuel failures due to high-temperature rupture for the case without void reactivity feedback is approximately ten times larger than the results obtained when the void reactivity feedback is taken into account. The void reactivity feedback becomes effective in the later phase of this event due to the delay of void generation at cold start-up condition, therefore the void reactivity feedback shows larger effect on the maximum fuel enthalpy and hence on the fuel failures due to high-temperature.

The results of three-dimensional analysis on control rod drop accident for EOC and CZP are summarized in Table 2. The results for the case with void reactivity feedback showed that the fuel safety criteria to avoid the core damage is adequately satisfied and the fraction of fuel failure is quite small under the control rod drop accident, even though the significant conservatism is employed in the dropped rod worth. As part of the analysis, the influence of a negative void reactivity feedback is studied. The results indicated that the void reactivity feedback greatly reduces the maximum fuel enthalpy and fuel failure for this event.

5.4 Results for a Core at EOC and HZP

The three dimensional analysis of control rod drop accident was performed for end of cycle (EOC) and at hot zero power (HZP). Fig. 12 shows the reactor power during the transient on a logarithmic scale relative to nominal power. The figure also shows the differences between the results with and without void reactivity feedback. For both cases, the power pulse started at about 1.0 seconds and reached a maximum value of 7.2 of nominal power at about 1.3 seconds. At that time, the power pulse was terminated due to the negative Doppler reactivity feedback. The power for the case with void reactivity feedback decreases gradually after termination of power pulse, while for the case without the void reactivity feedback, the power increase is continued until the plant is scrammed.

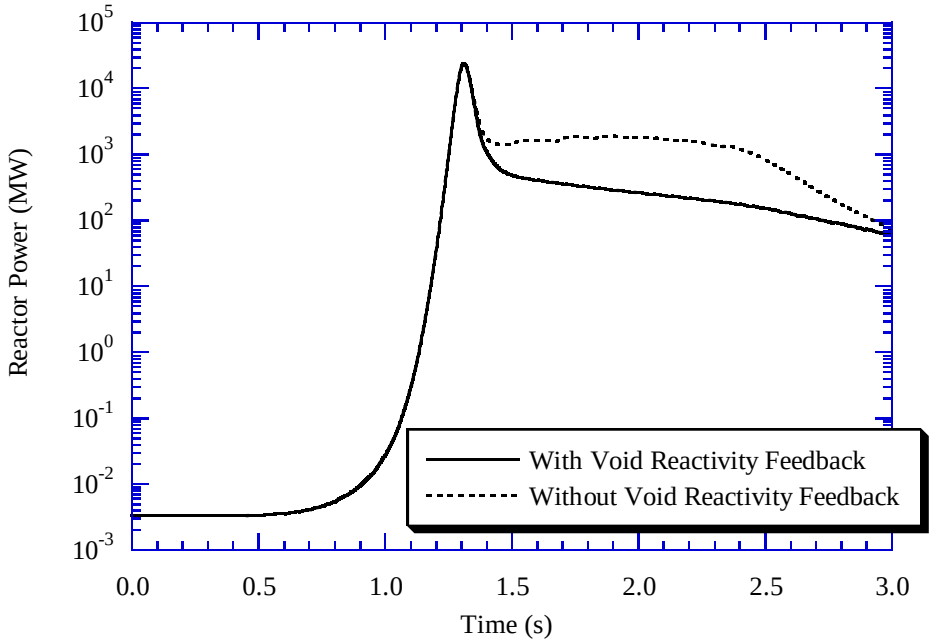

Fig. 12 Reactor power during the transient for EOC and HZP

Fig. 13 shows the trend of the different reactivity feedback components during the transient for the case with void reactivity feedback. The figure also shows the power pulse on a linear scale. This figure shows that the boiling in the core initiated right after the termination of power pulse and the void reactivity feedback acts significantly to reduce the power increase as shown in Fig. 12. In the hot standby condition, the coolant subcooling is very little and, therefore, the boiling begins immediately and a large amount of void can be generated in the assemblies surrounding the dropped rod.

Fig. 14 shows the maximum fuel enthalpy during the transient. The figure also shows the differences between the results with and without void reactivity feedback. For the case with void reactivity feedback, the fuel enthalpy increased rapidly due to the power pulse and reached a maximum value of 97 cal/g at about 1.4 seconds. At that time, the heatup due to the power pulse was terminated by the negative Doppler reactivity feedback and also the heatup after power pulse was suppressed by the void reactivity

feedback. While in the case without the void reactivity feedback, the fuel enthalpy still rises after termination of power pulse until the plant is scrammed and reaches a maximum value of 164 cal/g at about 2.8 seconds. These results indicate that the void reactivity feedback influences significantly to reduce the peak fuel enthalpy at hot stand-by condition.

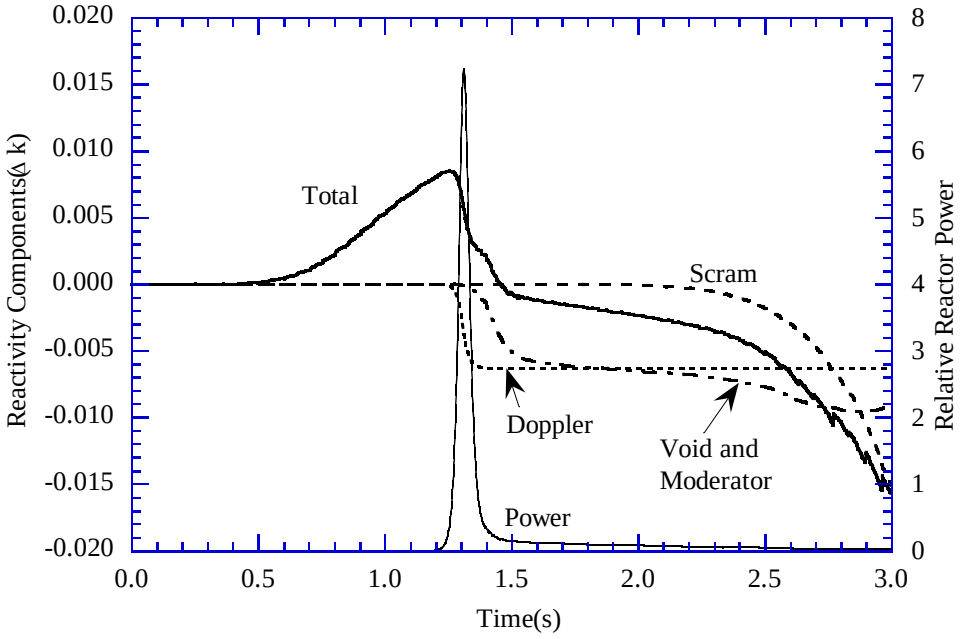

Fig. 13 Reactivity components during the transient for EOC and HZP

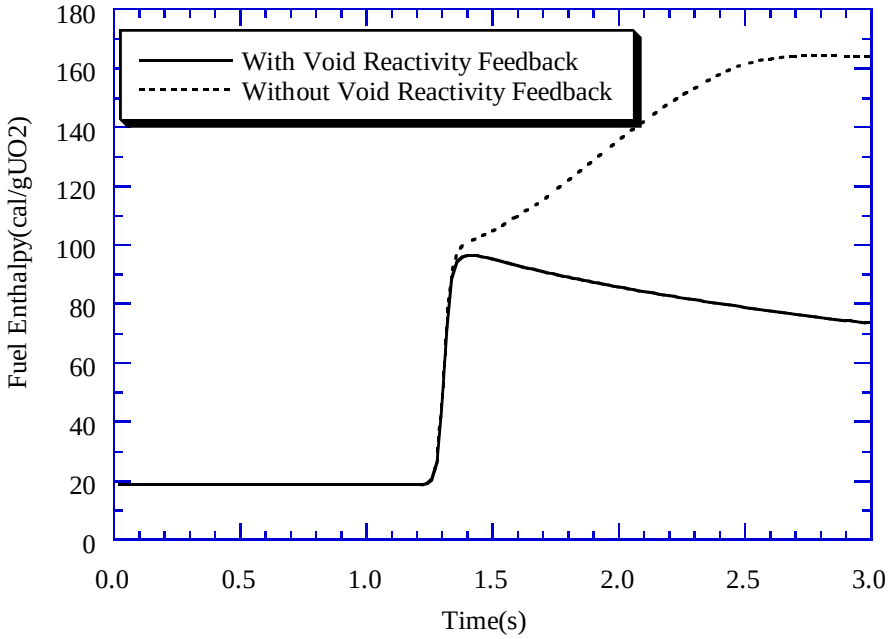

Fig. 14 Maximum fuel enthalpy during the transient for EOC and HZP

Fig. 15 shows the maximum fuel enthalpy distributions in the core. The maximum fuel enthalpy occurred in the one cycle burned fuel assembly adjacent to the dropped rod. The result indicates that the maximum fuel enthalpy in a assembly is correlated by the distance of the assembly from the dropped rod position, the control rod pattern and the burnup of the fuel.

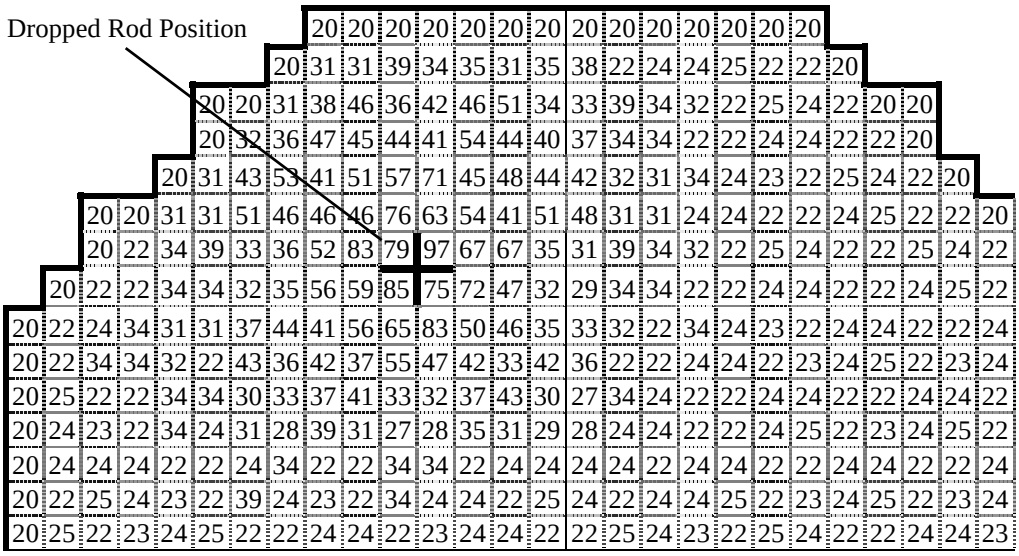

Fig. 15 Distribution of maximum fuel enthalpy of each assembly for EOC and HZP

Table 3 presents the numbers of fuel failures due to PCMI for the control rod drop accident. In Table 3, the difference between the results with and without void reactivity feedback is also compared. Since the initial fuel enthalpy increase at the time te defined in Fig.2 for two cases shows small difference, therefore, the difference between two cases for number of fuel failures due to PCMI is small. The void reactivity feedback becomes greatly effective in the later phase of this event at hot standby condition, therefore the void reactivity feedback shows smaller effect on the initial fuel enthalpy increase and hence on the fuel failures due to PCMI.

Table 3 Summary of the results performed for a BWR at EOC and HZP

Item	Results	
	With Void Reactivity Feedback	Without Void Reactivity Feedback
Maximum reactor power (ratio to nominal)	7.2	7.5
Maximum fuel enthalpy (cal/g)	97	164
Maximum initial fuel enthalpy increase (cal/g)	77	81
Number of fuel failures due to PCMI	26	49
Number of fuel failures due to high-temperature rupture	57	576

In contrast to the small difference for the results of fuel failure due to PCMI between the cases with and without void reactivity feedback, the large difference was obtained for the results of fuel failure due to high-temperature rupture between two cases as shown in Table 3. The maximum fuel enthalpy during the transient for the case without void reactivity feedback is about 85 % higher than the results with void reactivity feedback as shown in Fig. 14. Due to this difference, the number of fuel failures due to high-temperature rupture for the case without void reactivity feedback is approximately ten times larger than the results obtained when the void reactivity feedback is taken into account. The void reactivity feedback becomes greatly effective in the later phase of this event at hot standby condition, therefore the void reactivity feedback shows significant effect on the maximum fuel enthalpy and hence on the fuel failures due to high-temperature rupture.

The results of three-dimensional analysis on control rod drop accident for EOC and HZP are summarized in Table 3. The results for the case with void reactivity feedback showed that the fuel safety criteria to avoid the core damage is adequately satisfied and the fraction of fuel failure is less than 1% under the control rod drop accident, even though the significant conservatism is employed in the dropped rod worth. As part of the analysis, the influence of a negative void reactivity feedback is studied. The results indicated that the void reactivity feedback significantly reduces the maximum fuel enthalpy and fuel failure for this event.

5. Conclusions

The three-dimensional analyses of RIA for a typical BWR with high burnup fuel were performed using the EUREKA-JINS/S code to understand the realistic fuel behavior during the transient. The fraction of fuel failure was evaluated applying the newly revised failure threshold. For the analysis of RIA in BWR, the influence of void reactivity feedback was studied to understand how it affects on the fuel behavior under the RIA.

The results of three-dimensional analysis of control rod drop accident for a typical BWR showed that the fuel safety criteria to avoid the core damage is adequately satisfied and fuel failures are quite small under this event, even though the significant conservatism is employed in the dropped rod worth. As part of the analysis, the influence of a negative void reactivity feedback was studied. The results indicated that the void reactivity feedback greatly reduces the maximum fuel enthalpy and fuel failure for this event.

REFERENCES

Schmitz, F., et al., Investigation of the Behavior of High Burn-up PWR Fuel under RIA Conditions in the CABRI Test Reactor, Presented at the 22nd Water Reactor Safety Meeting, Washington, DC, October 1994.

Fuketa, T., et al., New Results from the NSRR Experiments with High Burnup Fuel, NUREG/CP-0149 vol.1, Presented at the 23rd Water Reactor Safety Information Meeting, October 1995.

NUPEC (JAPAN), Modification of Three Dimensional Neutronic Transient code EUREKA-JINS/S, INS/M97-06, March 1998.

Inabe, T., Ohnishi, N., Quasi Steady State Multi-Dimensional Space-Dependent Kinetic Code EUREKA-SPACE, Japan Atomic Energy Research Institute, JAERI-M7183, August 1977.

Nuclear Safety Commission in Japan, The Evaluation Guide for Reactivity Insertion Events of Light Water Nuclear Power Reactor Facilities, January 1984.

Fowler, T.B., Vondy, D.R., Cunningham, G.W., Nuclear Reactor Core Analysis Code: CITATION Revision 2, ORNL-TM-2496, July 1971.

Levy, S., Forced Convection Subcooled Boiling - Prediction of Vapor Volumetric Fraction, Int. J. of Heat & Mass Transfer, Vol.10, pp. 951-965, 1967.

Zuber, N., Findlay, J.A., Average Volumetric Concentration in Two-Phase Flow Systems, J. of Heat Transfer, Vol.87, pp. 453-466, 1965.

International Meeting on "Best-Estimate" Methods in Nuclear Installation Safety Analysis (BE-2000)
Washington, DC, November, 2000.

SATUS OF MODIFICATION AND VALIDATION OF BWR LOCA AUDIT ANALYSIS CODE AT NUPEC

Osamu YAMAMOTO Fumio KASAHARA and Ichiro KOMATSU
Institute of Nuclear Safety/Nuclear Power Engineering Corporation
Fujita Kanko Toranomon Bldg.,7F 17-1 3-chome Toranomon, Minato-ku, Tokyo Japan
S-YAMAMOTO@nupec.or.jp KASAHARA@nupec.or.jp KOMATSU@nupec.or.jp

Keywords: BWR, LOCA, Boiling Transition, audit analysis

ABSTRACT

In order to conduct audit analyses at the Institute of Nuclear Safety/Nuclear Power Engineering Corporation (INS/NUPEC), several physical models of RELAP5/MOD2 have been modified to improve the simulation capability for loss-of-coolant accidents (LOCA) in boiling water reactors (BWRs). The models modified are mainly related to the prediction of peak cladding temperature during the blowdown and reflood phases of a LOCA, e.g. models for inception of boiling transition, post-dryout heat transfer, interfacial friction, counter-current flow limitation (CCFL), CCFL breakdown, rewetting, spray water behavior, and two-phase mixture level. Systematic code verification of these models has been conducted using data from separate effect tests and integral tests. Some of the parameters sensitive to a BWR LOCA have been identified from these verification efforts, and they have been reflected in the modification of standard input data for the plant analysis. The enhanced code, named RELAP5/MOD2/INS, is used at NUPEC as the best estimate analysis tool for the BWR LOCA audit analysis.

1. INTRODUCTION

An audit analysis is one of the important missions of the Institute of Nuclear Safety/Nuclear Power Engineering Corporation (INS/NUPEC) in supporting the Japanese regulatory authorities with safety evaluations of nuclear power plant applications. The audit analysis codes at INS/NUPEC are based on frozen versions of open codes developed and evaluated by government organizations such as the United States Nuclear Regulatory Commission (USNRC), Japan Atomic Energy Research Institute (JAERI), etc. Initially, a modified version of RELAP4, namely RELAP4/MOD6/U4/J3, was introduced from JAERI and has been used at NUPEC as an audit analysis code for loss-of-coolant accidents (LOCA) for boiling water reactors (BWRs). Although most of the analysis models of the code had been validated before code transmission from JAERI to NUPEC, further modifications were found to be necessary. In particular, some BWR-specific components and phenomena were not modeled for LOCA analysis sufficiently to comply with the 1988 revision of the Japanese

"Guide for Evaluation of the Emergency Core Cooling System of LWR Power Plant" (ECCS assessment guideline). The main points of the revision of the Japanese ECCS assessment guideline are the certification of models and correlations proposed by the applicants and vendors based on their new experimental findings on CCFL, CCFL breakdown, by-pass leak flow etc.(Murase,1985), (Nagasaka,1984 and 1985). Because the models predicted peak cladding temperatures (PCT) drastically lower then those by the previous models, it was necessary to cope with these model changes. In the process of modification, several models based on confidential information of applicants and vendors had to be introduced due to the lack of available open information at that time. Thus there have been restrictions on disclose the details of the models to the public.

To avoid these restrictions and to improve the transparency and the analytical capability of the code, RELAP5/MOD2, the state-of the-art technology at that time, was introduced from the USNRC. However, experience with RELAP5/MOD2 showed that the code gave poor results when applying it to BWR LOCA analysis. For example, it tended to significantly overpredict both the void distribution and the amount of carry-over in two-phase flow. The causes of deficiencies were traced back to the original interfacial friction correlations used in the code, particularly those formulated for the bubbly and slug flow regimes. Efforts to correct such deficiencies are particularly important in BWR LOCA analysis since the deficiencies could cause poor prediction of the PCT. In order to remedy these deficiencies in RELAP5/MOD2, INS/NUPEC has incorporated a drift-flux based interfacial friction model for bubbly/slug flow.

The models to be verified are classified by taking into account the importance of the model parameters related to the LOCA acceptance criteria. Verification efforts have been carried out by using data from separate effect tests and integral tests. The following models have been qualified by using separate effect test data: interfacial drag, boiling transition, post-dryout heat transfer, counter-current flow limitation (CCFL), rewetting at reflood phase and spray water behavior. The integral performance of the code has been verified by using integral test data such as from the TLTA and the ROSA-III tests (Kasahara,1997 and 1998). The modified version of the code was named RELAP5/MOD2/INS and some of the parameters sensitive to the important phenomena have been identified and incorporated into the standard input data for actual plant analysis.

Generally, an uncertainty evaluation is necessary for the results obtained by BE code calculations. At present, we are in the investigation stage of a methodology and its effective usage for the uncertainty evaluation. Therefore, conservative analytical conditions will be used for audit analyses for the time being.

2. MODIFICATION AND VALIDATION FOR BWR LOCA ANALYSIS

The major process of a large break LOCA (LBLOCA) in BWR could be divided into two phases; namely blowdown phase and reflood phase. Many models for developmental assessment and for benchmarking with selected separate effect tests have been developed in the course of this work. The followings are the status of modification and validation of these two phases.

2.1 Blowdown phase

(1) Boiling transition

During the blowdown phase, the cladding temperature tends to increase because of a reduction of heat transfer coefficient caused by the rapid decrease in the core inlet flow rate. This phenomenon is called boiling transition (BT), which dominates the cladding temperature increase in the early stage of LBLOCA. As shown in Fig. 1, the ROSA-III LBLOCA simulation (Run926) by the tentative version of RELAP5/MOD2/INS did not predict the BT correctly. The initiation of BT is too early in Fig. 1 (a) and there is no sign of BT in Fig. 1 (b). The reason of these differences is the high sensitivity of critical heat flux (CHF) to the mass flux in the correlations included in original RELAP5/MOD2; Biasi's correlation (Collier,1972) for $G \geq 200 kg/m^2$-s and Modified Zuber correlation (Dongarra,1979) for $G \leq 100 kg/m^2$-s. If mass flux G is in between 100 and $200 kg/m^2$-s, a linear interpolation with respect to G is adopted to evaluate CHF. In the ROSA-III Run926 test, the mass flux decreases to around 100 kg/m^2-s and the corresponding CHF, which is very sensitive to the mass flux, is very close to the maximum heat flux of the core. Therefore the occurrence of BT depends on the flow rate (mass flux) evaluation in the core.

To improve the prediction capability of the inception of BT, a model using the critical power ratio (CPR) concept has been incorporated which is based on the CISE-type correlation fitted with the data of the NUPEC critical power experiments for the high-burnup 8x8 and the 9x9 A-type fuel assemblies (Mitsutake,1997) and (Kitamura,1998). To obtain the CPR, the average thermal equilibrium quality at each axial node in the flow channel of the fuel assembly is compared with the critical quality obtained at the same axial node by the correlation.

Figure 2 shows the comparison between the predicted and measured critical power of the high-burnup 8x8 steady state experiment. The overall relative prediction error is 4.6% on the standard deviation basis.

The correlation for high-burnup 8x8 fuel assembly was applied to the NUPEC transient experiment (Mitsutake,1997) in which the flow and power were changed as shown in Fig. 3. The cladding temperature histories at the upper part of the heat structure were compared with the experiment as shown in Fig. 4. The calculated temperature rise timing delays a little bit but it is within the acceptable range. This shows the good predictive capability of the incorporated model for the inception of BT.

(2) Post dryout heat transfer

As shown in Fig. 1(a), the post-dryout heat transfer correlation in the tentative version of RELAP5/MOD2/INS code gave relatively high cladding temperature for our experiences of application to several experiments. Therefore, a new post-dryout heat transfer correlation has been developed which takes into account the cooling effect of cladding surface by liquid droplets in the vapor stream. The correlation is formulated based on the Groeneveld film boiling equation (Groeneveld,1973) by adding the term which reflects the cooling effect by

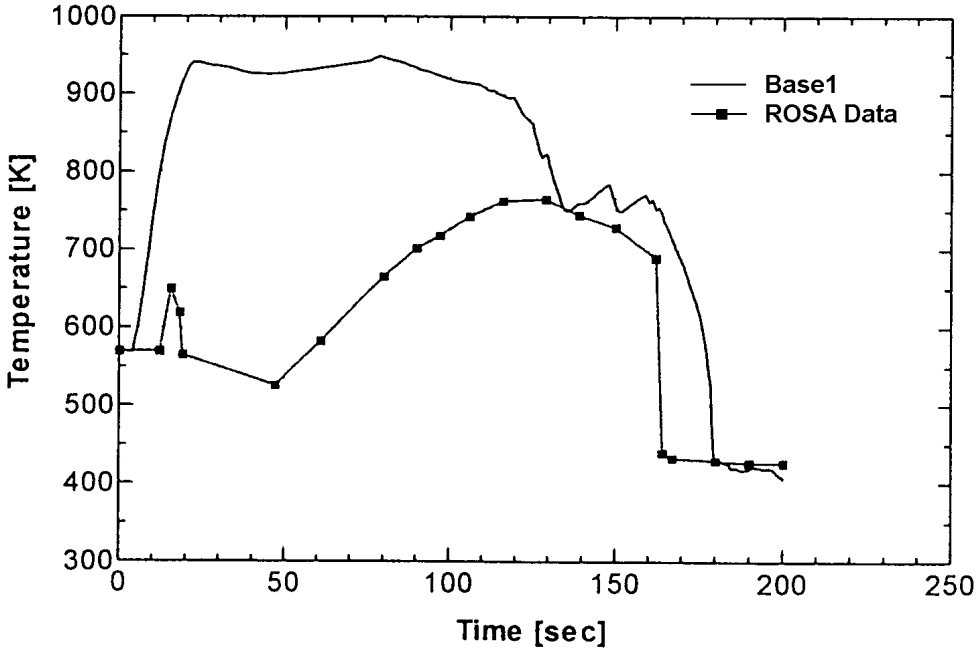

Fig.1(a) Cladding temperature comparison for ROSA-III (Run926) at axial position 3 calculated by RELAP5/MOD2/INS tentative version (Base case1)

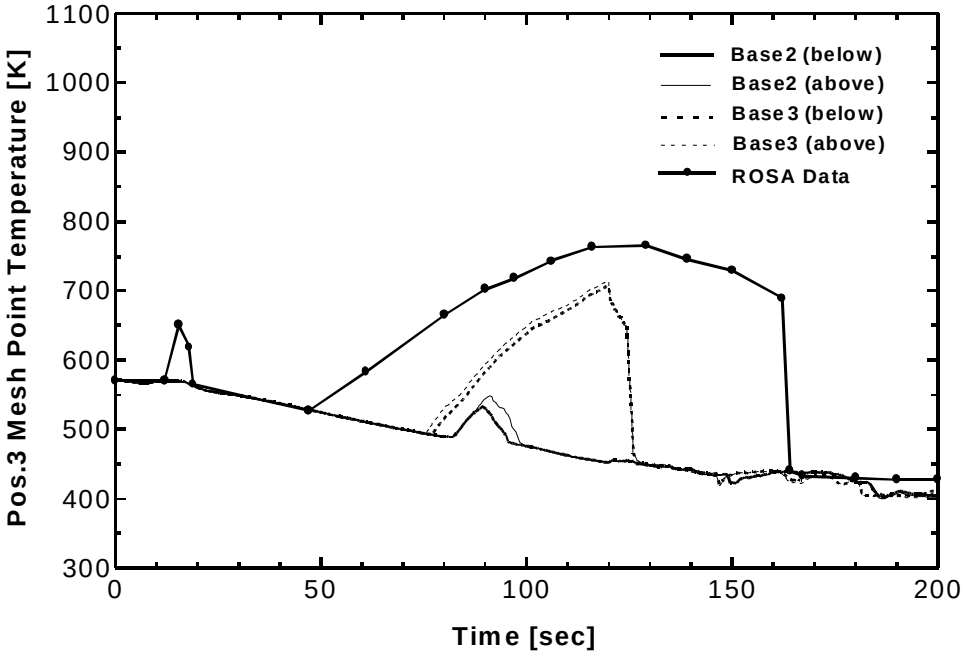

Fig.1(b) Cladding temperature comparison for ROSA-III (Run926) at axial position 3 calculated by RELAP5/MOD2/INS tentative version (Base case2 and 3)

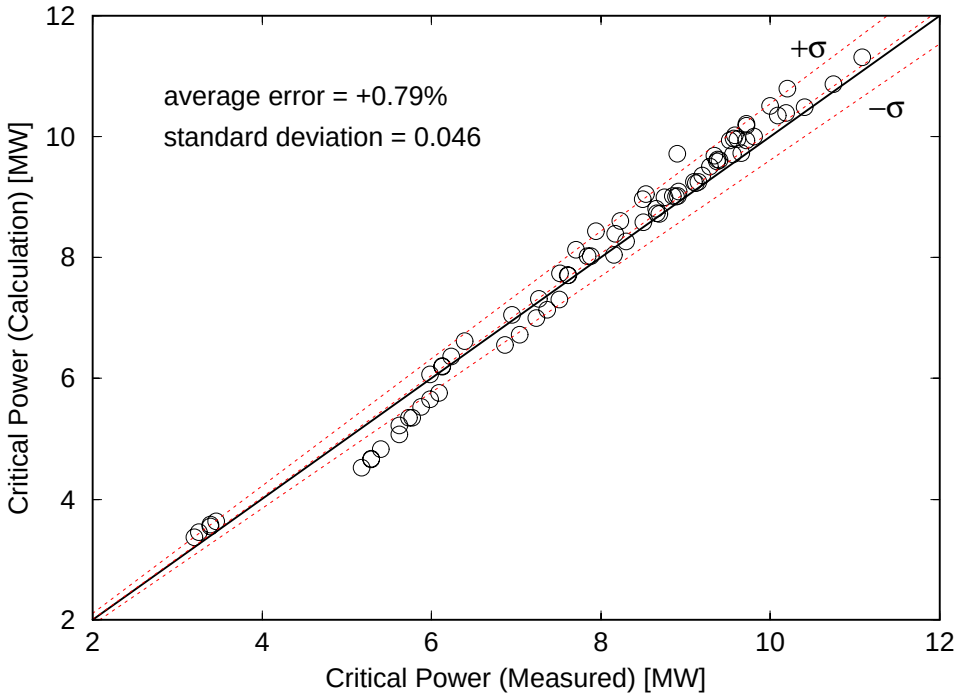

Fig.2 Critical power comparison between calculation and measurement

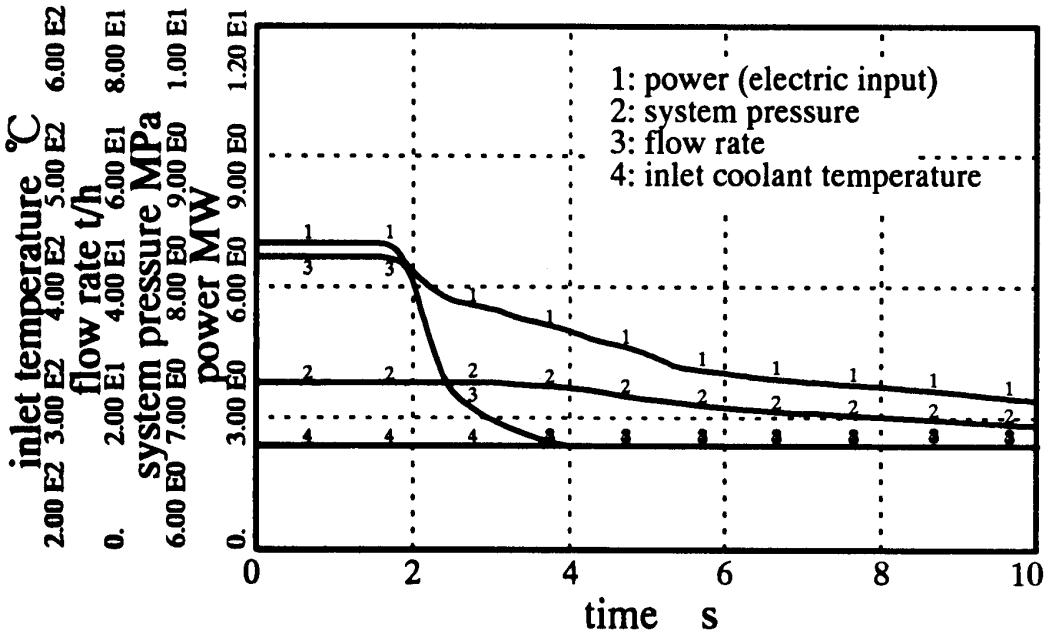

Fig.3 Transient data in the NUPEC experiment

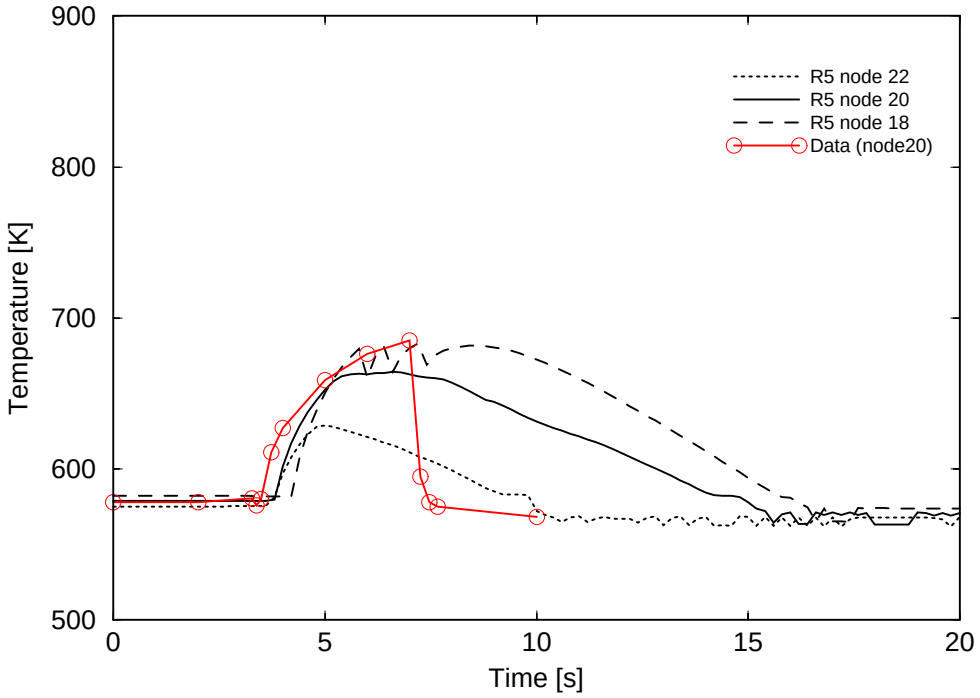

Fig.4 Cladding temperature response comparison for the NUPEC experiment

droplets from the data of the NUPEC transient experiment for the new-type 8x8 fuel assembly and the high burnup 8x8 fuel assembly respectively. Because the test section of the experiment simulated the full-scale fuel assembly for BWR and the experiments were held under the wide range of operating and accident conditions (though they don't cover the very low flow rate conditions), it was expected that the correlation gives better results than dose the original RELAP5/MOD2 model.

The temperature response shown in Fig. 4 is obtained by applying the post-dryout heat transfer model explained above. As shown in the Figure, the calculated increase rate and the peak value of temperature agree well with the experiment though the calculation does not simulate well the rewetting behavior. The rewetting condition in this calculation is given by the following conditions:

$$\text{MCPR} > 1 \text{ and } T_w < T_{min} \quad . \qquad (1)$$

Where T_w is the surface temperature of the cladding and T_{min} is the rewetting temperature calculated by Iloeje correlation (Iloeje,1995). Furthermore, even if the above condition is satisfied, the heat transfer coefficient follows the condition below;

nucleate boiling mode (if $T_w - T_{sat} < 45F$) , or

transition boiling mode (if $T_w - T_{sat} > 45F$).

Where T_{sat} is the saturation temperature of coolant. The slow decrease of the cladding temperature in Fig. 4 after the peak value is probably due to the shift of heat transfer mode from the post dryout to the transition boiling.

2.2 Reflood phase

In the reflood phase, the void distribution and the two-phase mixture level have serious importance for the prediction of PCT. Various phenomena such as pooling of water above the upper tie-plate and steam condensation in the upper plenum play an important role in determining when and how much the liquid penetrates the fuel bundle during the operation of core spray injection system. However, the up flow steam that has to pass through the upper tie-plate against the falling spray water affects this process. Thus, a CCFL situation can occur which, at sufficiently high steam velocity, results in little liquid downflow, i.e. "flooding".

The modification of the models has been performed to include above mentioned key phenomena: drift-flux based interfacial friction for bubbly/slug flow, CCFL for both saturated and subcooled fluid conditions, CCFL breakdown, rewetting at reflood phase, spray water behavior, and two-phase mixture level.

(1) Interfacial friction

INS/NUPEC traced the cause of overprediction of void distribution of the original interfacial friction correlations, particularly those formulated for the bubbly and slug flow regimes. In the original RELAP5/MOD2, the effect of void and velocity distributions among a local drag force and the effect of gradient of void distribution among a local interfacial shear force are not included. To improve these deficiencies, a drift-flux based interfacial friction model has been incorporated. The drift-flux correlations of Zuber-Findly (1965), Kataoka-Ishii (1987), Bestion (Analytis,1987), and EPRI (Chexal,1986) can be chosen depending on the geometry of the flow channel and flow rate.

The steady state boiling bundle uncovery experiment performed at the Thermal-Hydraulic Test Facility is used to see the applicability of the incorporated drift-flux model for the fuel bundle. Figure 5 shows the experimentally derived void-fraction profile overlaid with profiles computed by the original RELAP5/MOD2 interfacial friction model and the three new models mentioned above. The experimental result shows that fluid enters with zero void due to its subcooling and then void fraction increases with elevation in a relatively linear or slightly parabolic manner. At a location near the two-phase mixture level, a sharp increase of void fraction with elevation occurs. In this region, void fraction rapidly approaches 1.0 and region of steam-cooling is reached. The EPRI and the Bestion drift-flux correlations provide very good improvement over the unmodified RELAP5/MOD2 and Kataoka-Ishii models. Though all correlations (including the original one) predict steeper transition at the steam-cooling region than the suggestion of experimental data, further improvement has not been attempted currently because the results shown in Fig. 4 give conservative results for PCT evaluation.

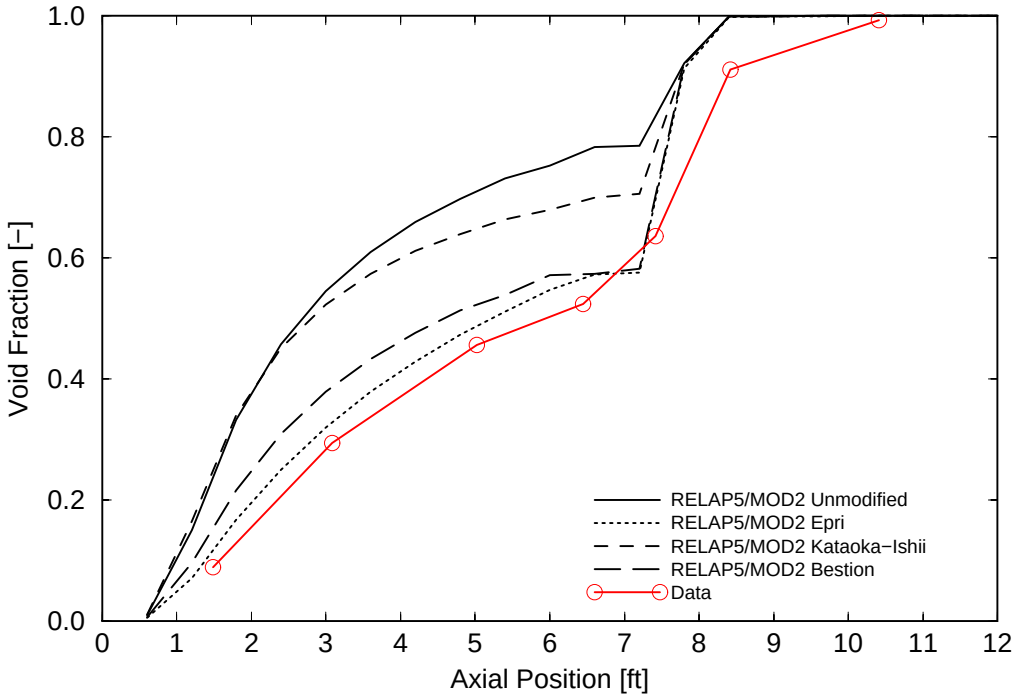

Fig.5 Void distribution comparison for the THTF experiment

(2) Counter current flow limitation (CCFL)

Without CCFL model, the current system code could not adequately predict coolant distribution in certain special situations such as core spray flooding at the upper tie-plate of BWR fuel channels. Because this phenomenon depends highly on the geometry where it occurs, different models are incorporated into the code: upper tie plate CCFL, bundle inlet CCFL, side entry orifice (SEO) CCFL, and bypass channel CCFL, respectively. Three types of correlations Wallis (1980), Kutateladze (1972), and Bankoff (1981) can be chosen in each model.

The upper tie plate and the bundle inlet CCFL models have been qualified against experimental CCFL data obtained for mixtures of air-water and steam-water. Calculations are performed for both general geometry (air-water experiment in a pipe (Dukler and Smith,1979)) and BWR specific geometry (steam-water experiment in an 8x8 bundle (Jones,1977)), respectively (Kasahara,1997).

Figure 6 (a) and (b) show the results of calculation for air-water experiment with and without the CCFL model. The experimental data are shown for comparison. The Wallis type of CCFL correlation expressed below is used with m=1.0 and C=0.88;

$$K_g^{1/2} + m K_f^{1/2} = C \qquad (2)$$

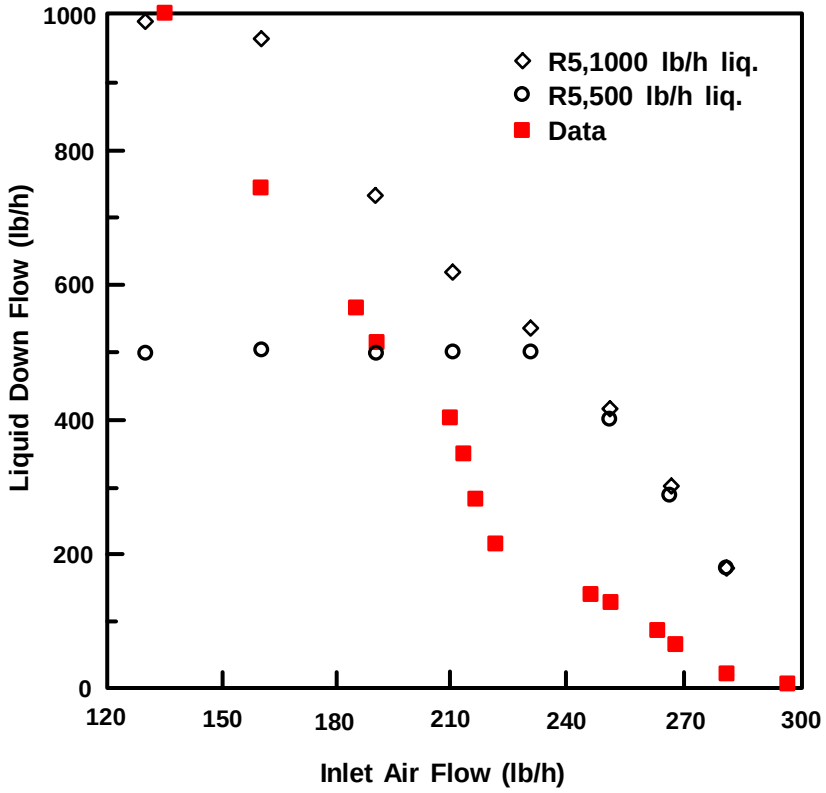

Fig.6 (a) Comparison with no CCFL model for the Dukler & Smith experiment

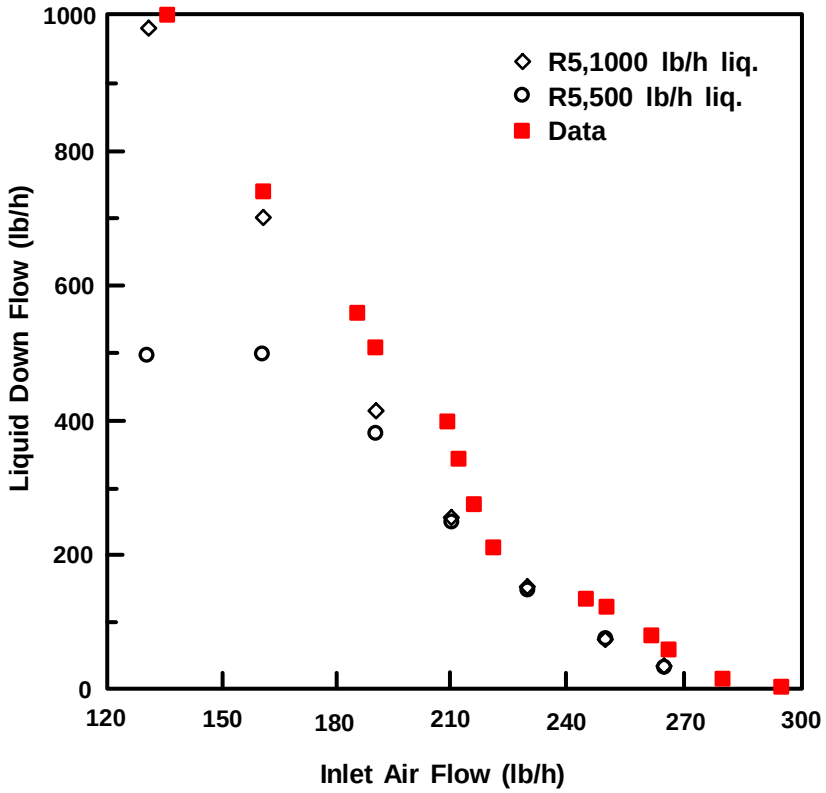

Fig.6 (b) Comparison with CCFL model for the Dukler & Smith experiment

Where m and C are constants, K_g and K_f are non-dimensional mass flux of gas and liquid, respectively. The result without CCFL model shows the poor prediction for liquid down flow, whereas much better agreement with the experimental data is obtained when the CCFL model was incorporated.

The existing CCFL correlations for side-entry orifice (SEO) and by-pass channel were modified by reflecting their structures. Only a qualitative validation was performed because there are few experiments that directly cover the whole BWR specific geometry where the CCFL may occur.

(3) CCFL breakdown

The phenomenon of CCFL breakdown is defined as the accumulation of cold spray water in the local peripheral region of the upper plenum breaks the CCFL and penetrates into the peripheral fuel channels. The model is the same as the CCFL models shown above but the subcooling effect of the cold spray water is taken into the correlation. Therefore an experiment (Sun,1979) was chosen that equipped with the upper plenum section, where saturated or subcooled water was sprayed on the top of 8x8 BWR bundle and steam flows upwards. Figure 7 compares the subcooled CCFL model with the experimental observations. It shows that the calculations slightly overestimate the liquid down flow.

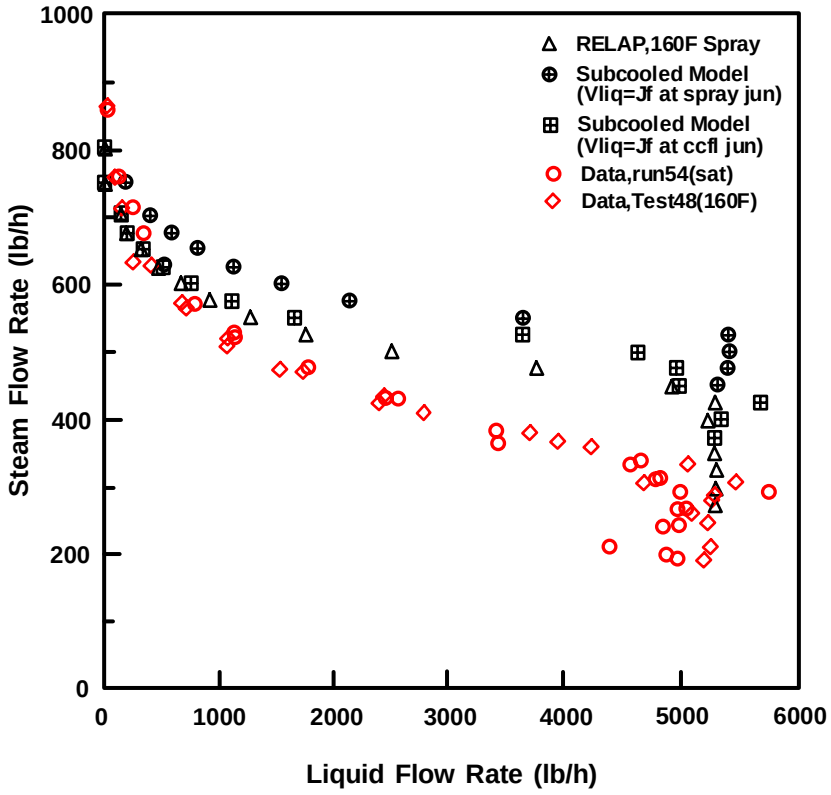

Fig.7 Subcooled CCFL model comparison for the Jones experiment

(4) Rewetting during reflood phase

Rewetting during reflood phase has much influence on the second peak of cladding temperature occurring in the reflood phase. As shown Fig. 1(a), the ROSA-III experimental analyses using original rewetting model show that there occurs no rewetting after the BT during blowdown phase and the timing of rewetting in the reflood phase is delayed compared with the experimental observations. The reason seems that the rewetting temperature is too low. Another observation gained in the experimental analyses is the abrupt change of the calculated void fraction near the quench front. This was confirmed to be due to the drastic change of the interfacial friction value that depends on the flow regimes. Therefore, following modifications are implemented into the code to improve the simulation capability of the rewetting during reflood phase;

i) Modification of the value of constant ε of the Weisman transition boiling heat transfer coefficient (Weisman,1981) (Eq.3) to obtain higher value than that obtained by the original correlation. This modification improves the prediction of the rewet timing.

$$
\begin{aligned}
&h_{TB} = h_m \exp(-\varepsilon \Delta T) + 4500 (G / G_{ref})^{0.2} \exp(-0.012 \Delta T) \\
&\text{Where } h_m \text{ and } \Delta T \text{ are} \\
&h_m = q_{cr} / \Delta t \\
&\Delta T = T_w - T_{sat} - \Delta T_m \\
&\text{respectively. Where} \\
&\Delta T_m = S (q_{cr} / 2.235)^{1/3.86}
\end{aligned}
\qquad (3)
$$

The term S is Chen's boiling suppression factor, q_{cr} is critical heat flux, G is mass flux, T_w is wall surface temperature, T_{sat} is saturation temperature of coolant, respectively. The value of ε was changed from 0.04 to 0.017.

ii) Modification of the criteria for the change of the interfacial friction correlation to correct the void fraction discontinuity near the quench front.

iii) Introduction of the constant rewetting temperature option (800K) to increase the rewetting temperature in order to improve the discrepancy of quench time between the calculations and experiments.

iv) Adoption of the Bestion's drift-flux correlation to improve the void fraction discontinuity near the quench front, because the interfacial friction evaluated using this correlation does not chang so much under the flow regime change at the occurrence of quench.

These modifications are based on the experiences of the analyses for the FLECHT (Hassan,1986) and NEPTUN (Grutter,1981) experiments (Kasahara,1997).

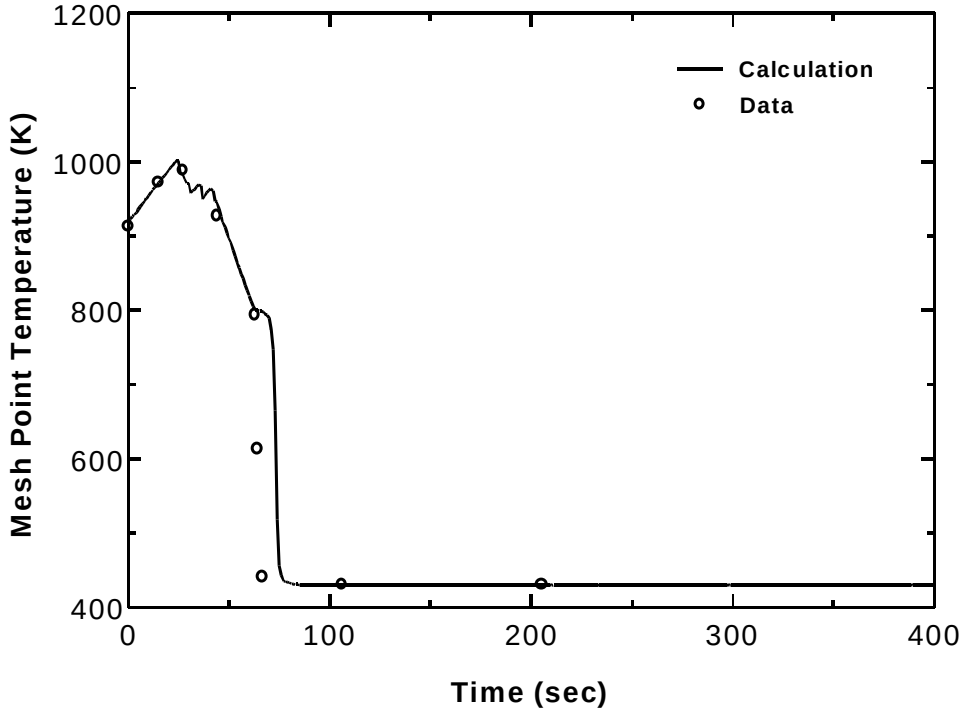

Fig.8 (a) Cladding temperature comparison at level 3 for the NUPTUN test

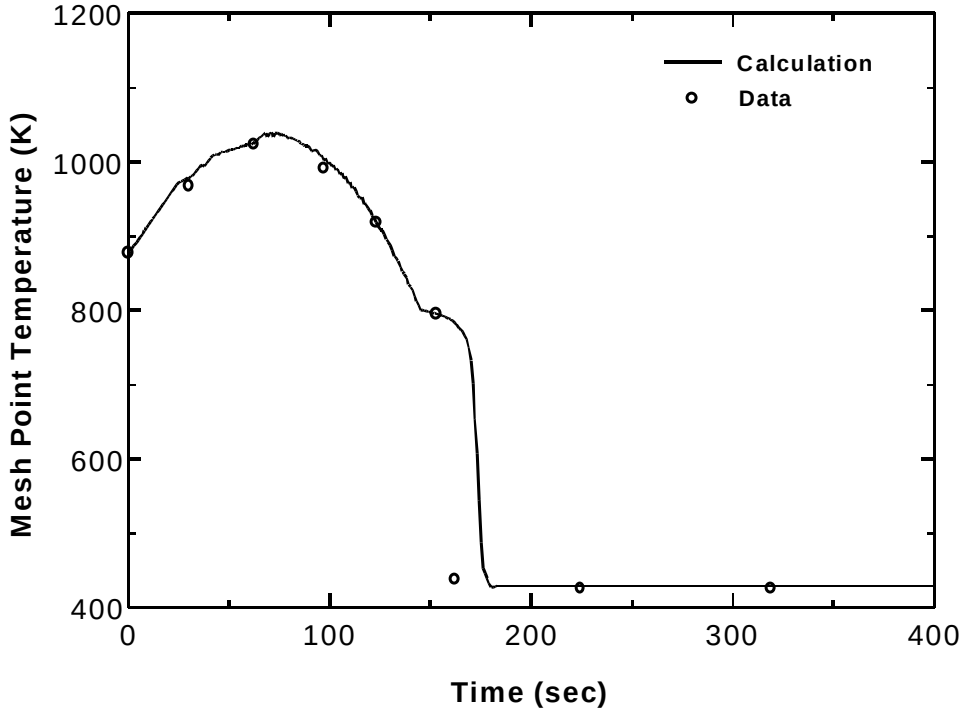

Fig.8 (b) Cladding temperature comparison at level 5 for the NUPTUN test

The modified rewetting model in the reflood phase was qualified by comparing the calculated cladding temperatures with those obtained from the experiments. The results of the analyses for NEPTUN experiments are shown in Fig. 8. The agreement is quite well and the implemented models are confirmed to be useful to predict the rewetting during reflood phase. The other example is the analysis for the FLECHT experiments. Figure 9 shows the cladding temperature history at different axial locations. By the application of constant value for the rewetting temperature and the heat transfer coefficient of Weisman transition boiling correlation, the better agreement for the quench time is obtained between the calculation and experiments.

(5) Spray water behavior

The CCFL and CCFL breakdown behaviors on the top of fuel assemblies strongly depend on the radial location of fuel assembly in the core. This is due to the inhomogeneous distribution of spray water in the upper plenum. To simulate inhomogeneous spray water distribution, a two-dimensional multi-volume treatment of upper plenum (hereafter calls UPM: Upper Plenum Model) was incorporated in which the upper plenum is divided axially and radially into several volumes as shown in Fig. 10.

The UPM model was qualified by comparing the calculated results with the SSTF experiments (1981). The analytical geometry is shown in Fig. 10. The experiment is a full-scale mock-up of BWR/6 with 1/12 symmetry in which high/low pressure spray systems (HPCS/LPCS) and low pressure coolant injection system (LPCI) are installed at the upper plenum section. Some of the SSTF EA1 series experiments were analyzed. Eleven tests were performed and they are divided into three groups depending on the system pressure. The test conditions are listed in Table 1. The initial water level is maintained with spraying the saturated water into the upper plenum. Then the transient starts with spraying the subcooled water instead of the saturated water. The test continues until the water level reaches the final stable level. In the analysis, duration of null transient by spraying the saturated water until the expected water level (~40sec) sets the initial condition. Then the spray water condition is changed from saturation to subcooling. Those values of final water level, discharged time (time between the water level changes from the initial to final level), and water temperature at the upper tie-plate are compared with the experiment, respectively. Figure 11 shows the axial water flow, the collapsed water level, and the water temperature at the three regions in the upper plenum (inner, middle, and outer regions), respectively. It can be seen that the typical CCFL breakdown characteristics such as downward flow of subcooled water and leveling of collapsed water after the CCFL breakdown. The results are shown in Table 2. The examination of all the results show that the predicted discharged time is acceptable though it is a little bit earlier than that of the measurements. The calculated final collapsed water level is evaluated to be a little bit higher than measurements, however, relative difference between analyses and measurements are reasonable by taking into account the effect of static head and form loss of the tie-plate on the driving force of the downward motion of subcooled water into the fuel assembly.

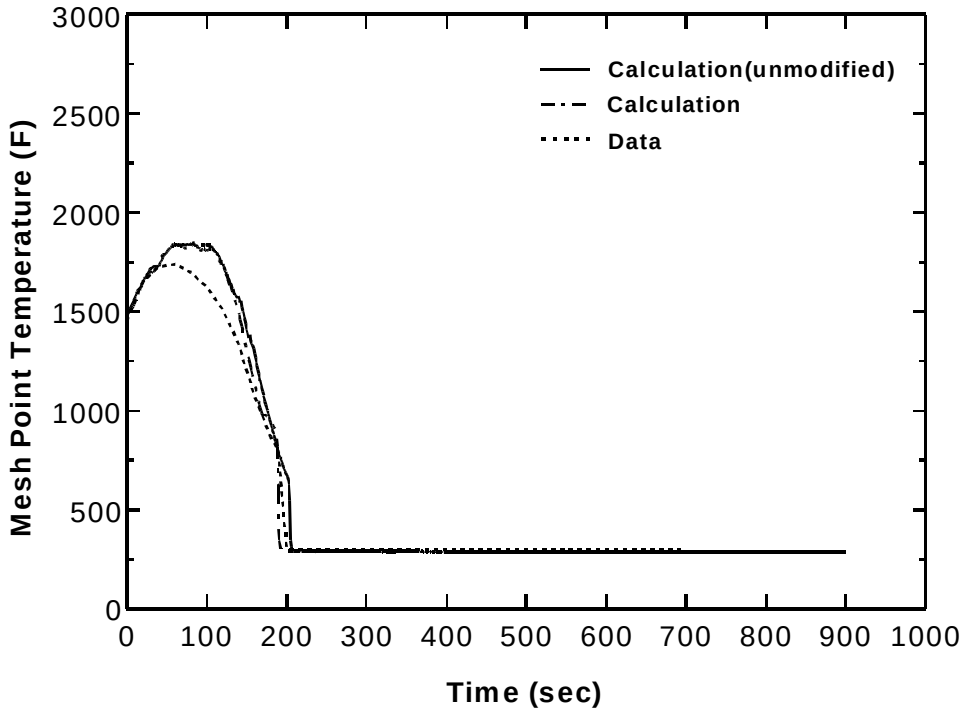

Fig.9(a) Cladding temperature comparison at 4ft from the bottom for the FLECHT test

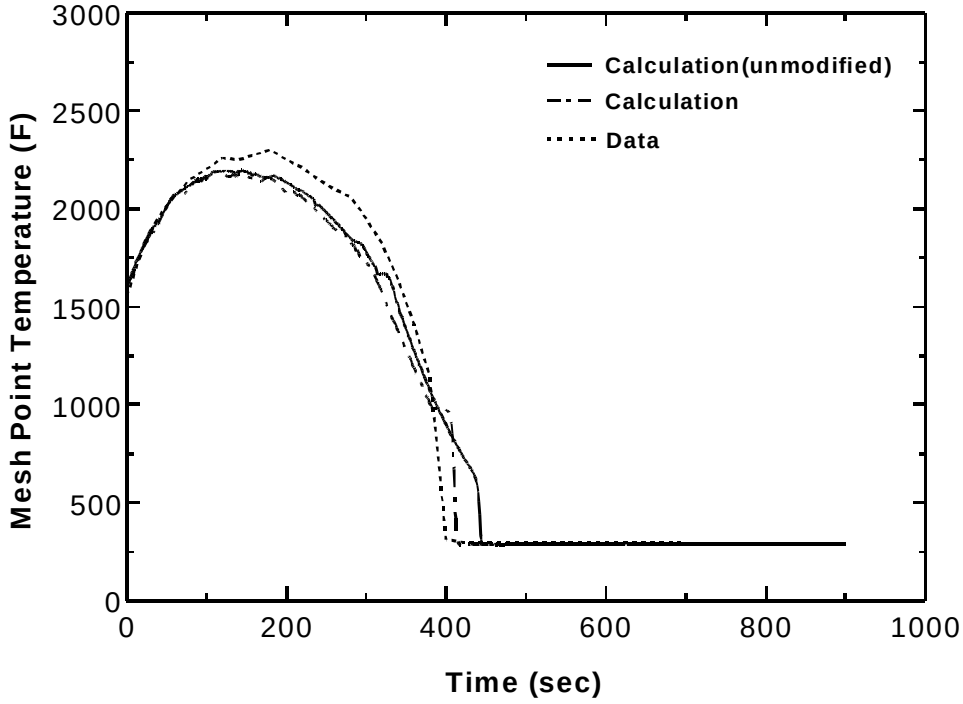

Fig.9(b) Cladding temperature comparison at 6.5ft from the bottom for the FLECHT test

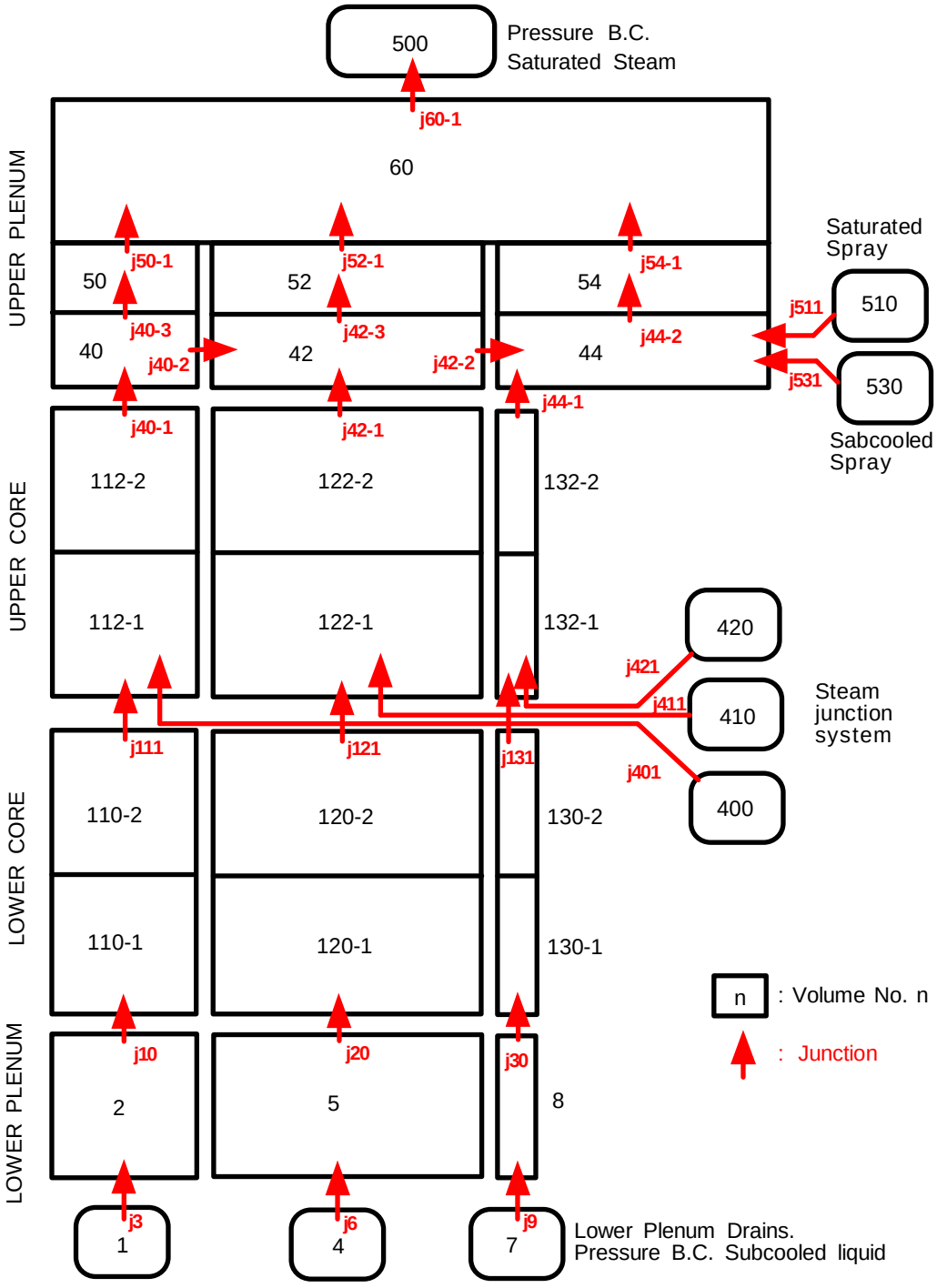

Fig.10 Analytical model for the SSTF experiment

Table 1 Test condition of SSTF EA1 TEST series

No.	P [psia]	Tsat [F]	Wvap [lb/hr]	Wspray [gpm]	Tspray [F]	Linit [inch]	Lfinal [inch]	Tdis [sec]	Tfinal [F]
1	29.5	247	40700	493	98	13.2	2.2	24	217-226
2				497	124	12.8	1.0	29	220-230
3				499	149	12.9	1.1	43	228-236
4	73.5	306	59700	449	101	16.8	1.6	28	287-300
5			59900	443	147	14.4	1.2	35	295-300
8			60000	449	104	8.4	1.9	12	288-300
9			60600		97	0.0	1.5	N/A	291-300
6	150.	359	73000	358	106	19.4	0.9	31	350-359
7			73600		147	18.5	0.0	42	349-359
10			73100		101	0.0	0.0	N/A	355-359
11			73700		144	0.0	0.0		349-359

The blank box means the corresponding value is the same as above box

P :pressure
Tsat :saturation temperature of water
Wvap :mass velocity of vapor
Wspray :volume velocity of spray
Tspray :spray water temperature
Linit :initial water level
Lfinal :final stable water level
Tdis :discharged time
Tfinal :final water temperature at upper tie-plate

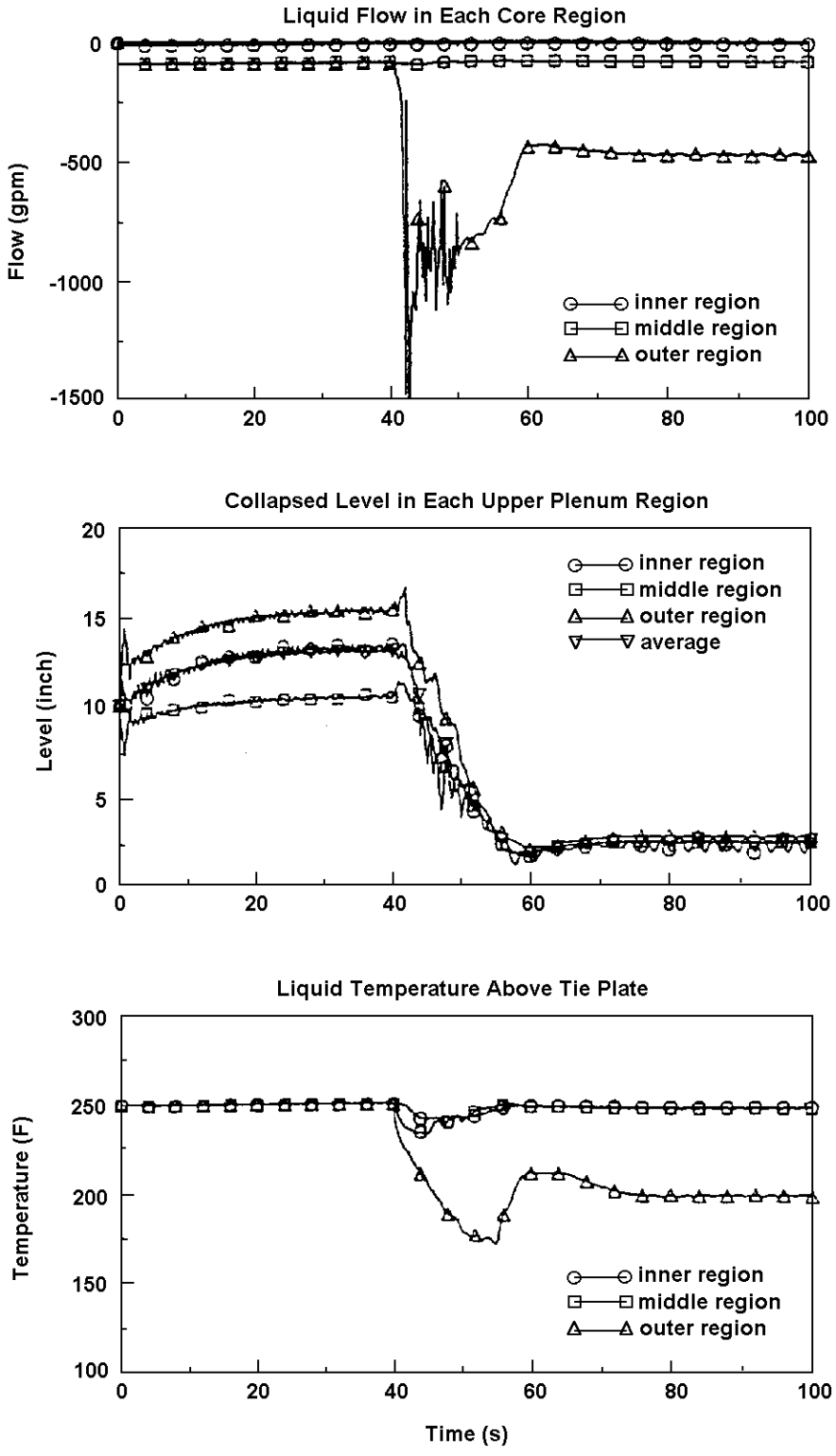

Fig.11 Comparison of variables for the EA1-1 test in the SSTF experiment

Table 2 Comparison between the analysis and measurement for SSTF EA1 TEST series

No.	Lfinal [inch]		Tdis [sec]		Tfinal [F]	
	Calculation	Experiment	Calculation	Experiment	Calculation	Experiment
1	2.8	2.2	19	24	199	217-226
2		1.0	20	29	208	220-230
3		1.1	40	43	216	228-236
4	2.8	1.6	23	28	251	287-299
5	3.0	1.2	25	35	259	295-300
8	3.0	1.9	10	12	251	288-300
9	2.7	1.5	N/A	N/A	254	291-300
6	2.4	0.9	27	31	309	350-359
7	3.0	0.0	30	42	301	349-359
10	2.3	0.0	N/A	N/A	309	355-359
11	2.7	0.0			312	349-359

The blank box means the corresponding value is the same as above box

Lfinal :final stable water level
Tdis :discharged time
Tfinal :final water temperature at upper tie-plate

(6) Two-phase mixture level

There is no model to calculate the two-phase mixture level in the original RELAP5/MOD2. However, the precise modeling of the two-phase mixture level is expected to be useful to examine the reason of clad temperature change during the LOCA and it may influence the mass flow rate above and below the two-phase mixture level. Therefore, several models are incorporated into the code: the drift flux based model, the bubble rise velocity based model, and the doner cell based model.For the qualification of the two-phase mixture model, the analysis of the GE level swell experiments (Anklam,1982) were performed. First, the sensitivity of interfacial friction correlation of the two-phase mixture level was examined for the small vessel experiment without reflecting the mixture density jump condition to the mass balance calculation. The correlation based on the Kataoka-Ishii (1987) gave a better agreement with the measurement than others as shown in Fig. 12. Thus the correlation of Kataoka-Ishii was adopted for the experiment analysis. Figures 13(a) and (b) show the two-phase mixture level calculated for large- and small- vessel experiments, respectively. In the case of small vessel experiments (Fig.13 (b)) the calculations show the close agreement with the measurements and any model gives the similar results. However, in the case of large vessel experiments (Fig.13 (a)) the calculated mixture level is systematically underestimated the experimental value. One of the reasons may be due to the fact that the non-equilibrium effect is strong in the large vessel experiment whereas the model correlation is based on the

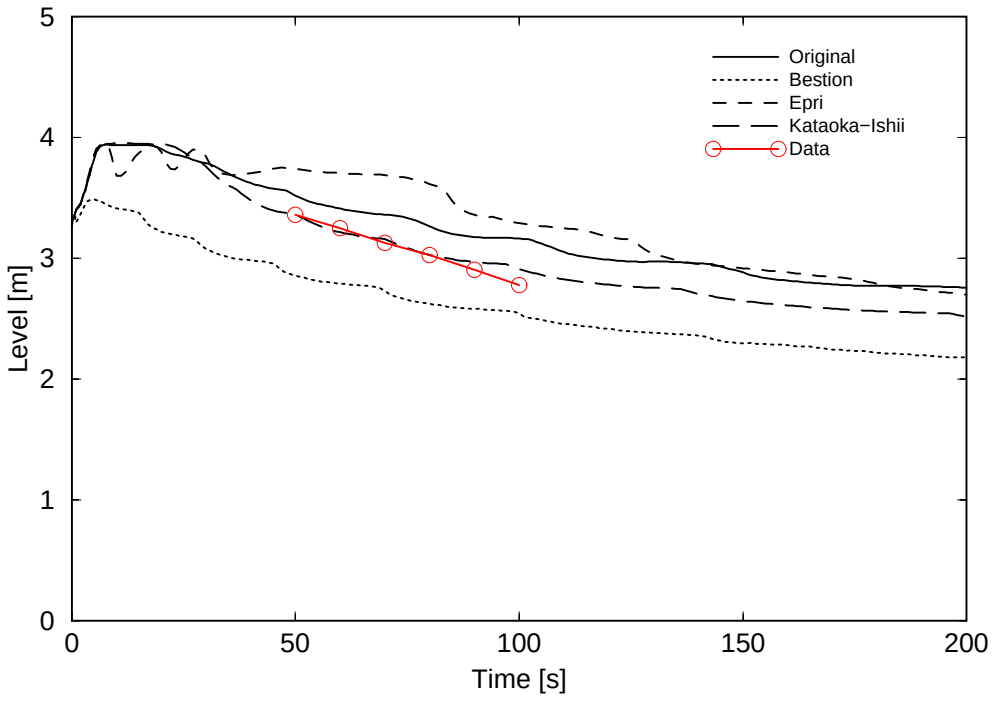

Fig.12 Two-phase mixture level comparison for the GE small vessel experiment (Effect of interface friction model difference)

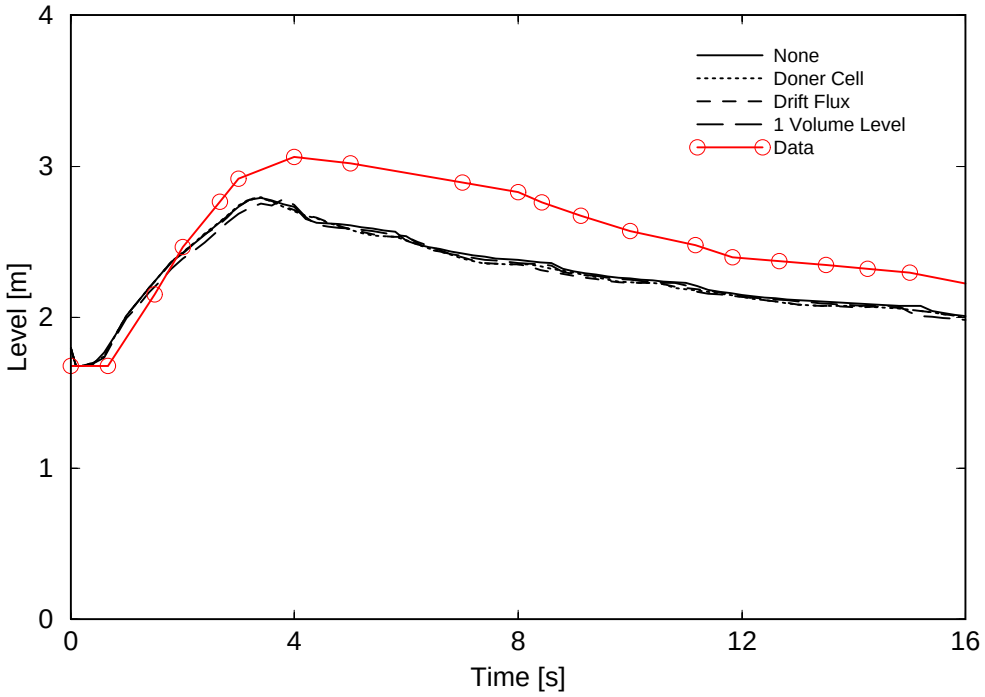

Fig.13(a) Two-phase mixture level comparison for the GE large vessel experiment (Effect of mixture level model difference)

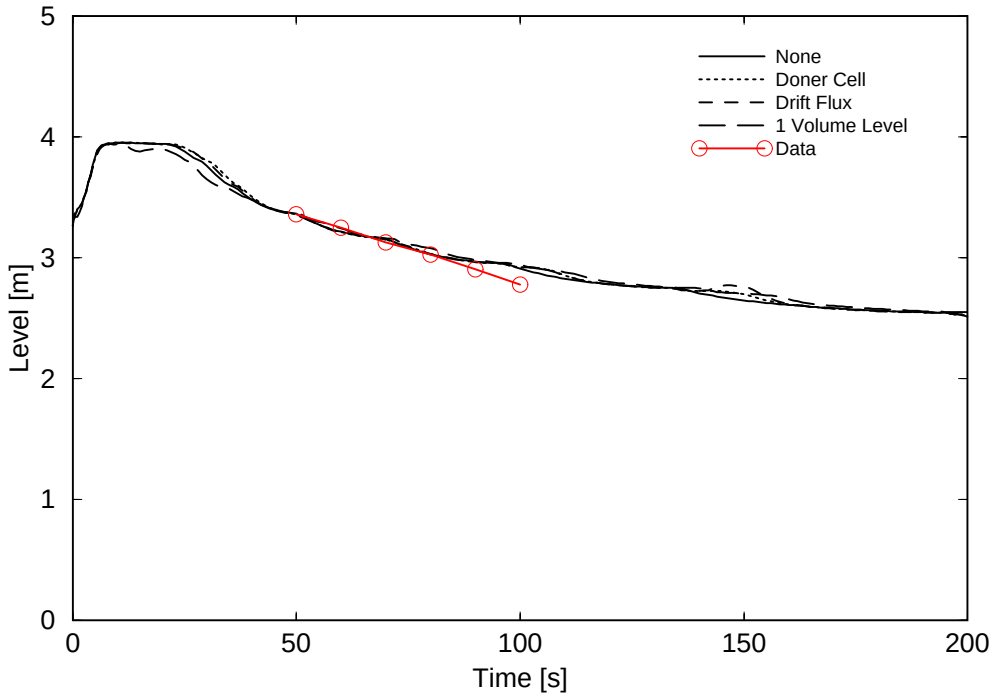

Fig.13(b) Two-phase mixture level comparison for the GE small vessel experiment (Effect of mixture level model difference

steady state equilibrium condition. For the safety point of view, the underestimation of the mixture level is conservative for the evaluation of clad temperature. Therefore, INS/NUPEC doesn't intend to modify the model further to improve the prediction capability of the mixture level.

3. VERIFICATION AGAINST INTEGRAL TEST

In the previous chapter it is shown that both the modified models and the implemented correlations represent a significant improvement over the original version of the RELAP5/MOD2 code. Therefore, this modified version named RELAP5/MOD2/INS is expected to notably contribute to performance of "Best-estimate" analysis.

The integral performance of the RELAP5/MOD2/INS code has been verified against the tests such as the TLTA (Lee,1982) and the ROSA-III (Nakamura,1984), which simulate the transients under the various pipe rupture conditions. The TLTA is the experiment simulating the large- and small-break LOCA in BWR-6 with a scale of 1/624. The experimental apparatus is equipped with fundamental components of BWR in which one full-scale heated bundle simulates the core. The analysis model for the TLTA-5A is shown in Fig. 14. A flow junction to simulate the leak flow and the CCFL is disposed between the bypass (V30) and the core inlet (V15) because their influence on the LOCA hydraulics is large. The calculated clad temperature histories at the axial node 2 and 5 in the core (V20 in Fig. 14) are compared with the measurements of the TLTA-5A/6424 (LBLOCA) in Fig. 15. The plural curves represent the data from the same axial location. The calculations give conservative results because the timing of temperature rise is relatively earlier and the peak temperature is higher than those of the experiment.

The ROSA-III is the experiment to simulate the large- and small- break LOCA in BWR with a volume ratio of 1/424. The core consists of four 8x8 heater pin bundles with a half height of full-scale ones. The analysis model is shown in Fig. 16. The calculations were performed to simulate the small break (5%) LOCA (SBLOCA) experiment Run912 by changing the interfacial friction model, the tow-phase mixture level model, and the noding of lower and upper plenums to their sensitivities. The calculation cases are listed in Table 3. Case 1 (Reference Case) applies the Kataoka-Ishii's interface friction model, and the two-phase mixture level model is added to Case 2. The original interface friction model is used instead of Kataoka-Ishii's in Case 3. The difference between Case 2 and Case 4 or Case 5 is that one node lower plenum model is used in Case 4 and one node upper plenum model is used in Case 5, respectively. Figures from 17 to 19 compare the history of pressures at the top of the pressure vessel, the collapsed water levels in the downcomer, and the PCTs for the calculation cases listed in Table 3 and the measurements, respectively. These results show that the modification of interfacial friction model and the incorporation of two-phase mixture model does not influence much to the overall behavior in SBLOCA, though the PCTs are higher and the rewetting occurs later in the Cases with incorporated models than in the Case of original interfacial friction (Case 3). However, the overall trend (the delay in the initiation of the cladding temperature rise, under prediction of PCT and earlier rewetting) of peak cladding temperature in Fig. 19 is non-conservative from the point of view of safety analysis. These trends are also seen in the RELAP5/MOD2/INS calculation of ROSA-III LBLOCA test

RUN926 as shown in Fig. 1. One of the reasons of these trend is the amount of water remained in the core is slightly larger in the calculation than in the experiment. Further qualification effort is in progress to obtain conservative results in ROSA-III test.

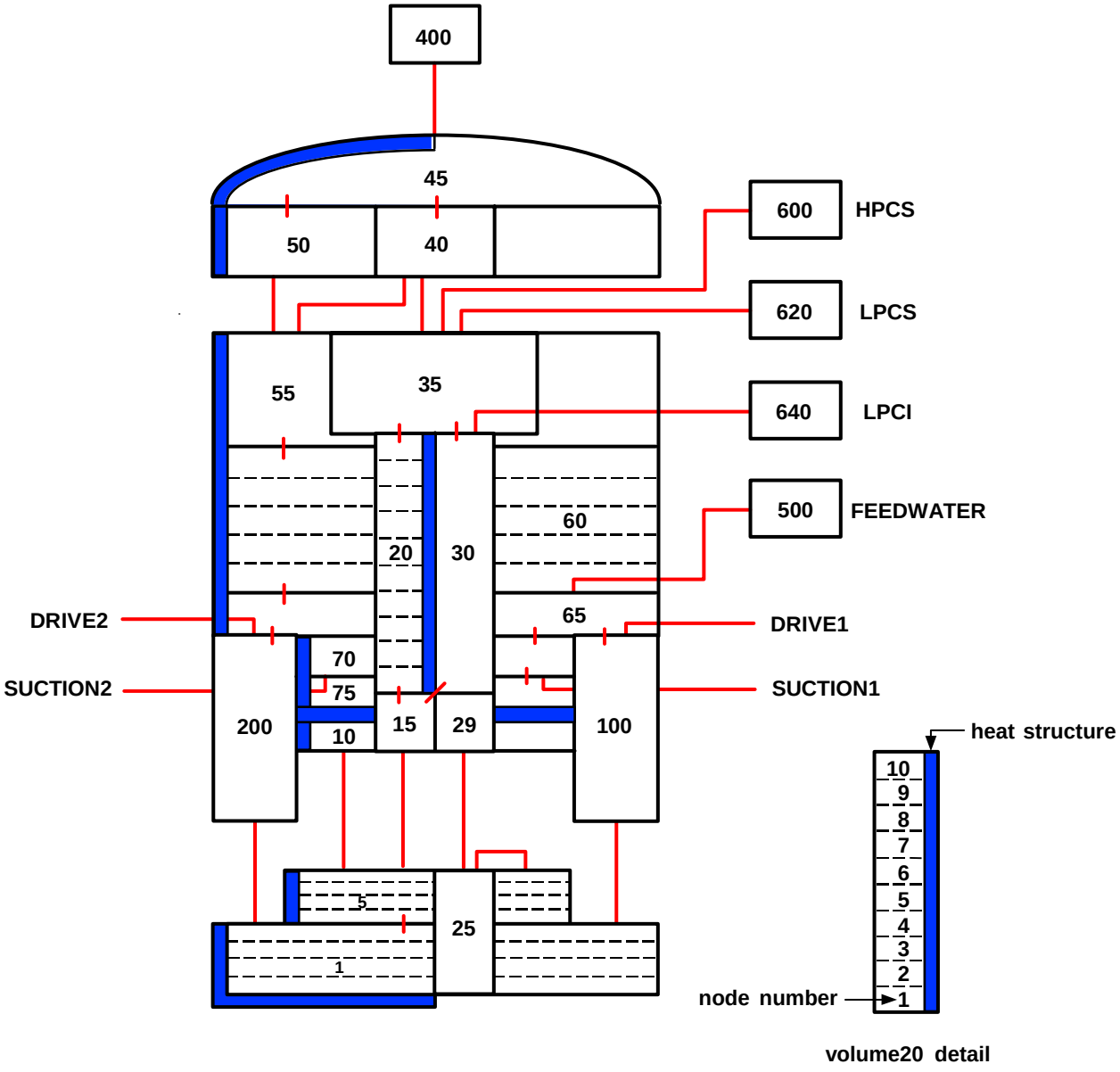

Fig.14 Vessel model for the TLTA-5A

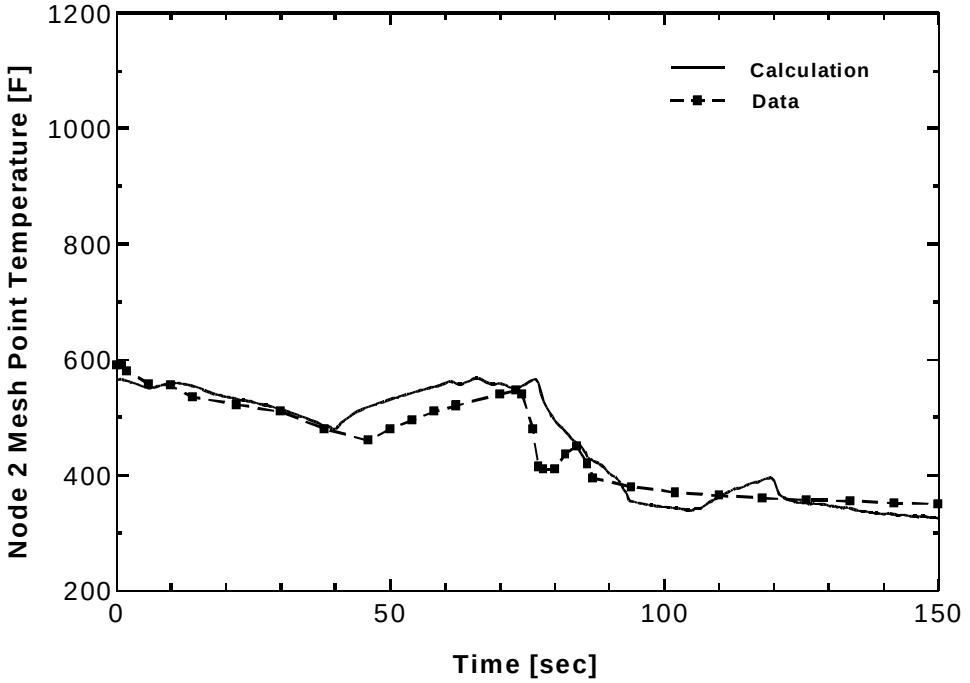

Fig.15(a) Cladding temperature comparison at node 2 for the TLTA-5A/6424 RUN1

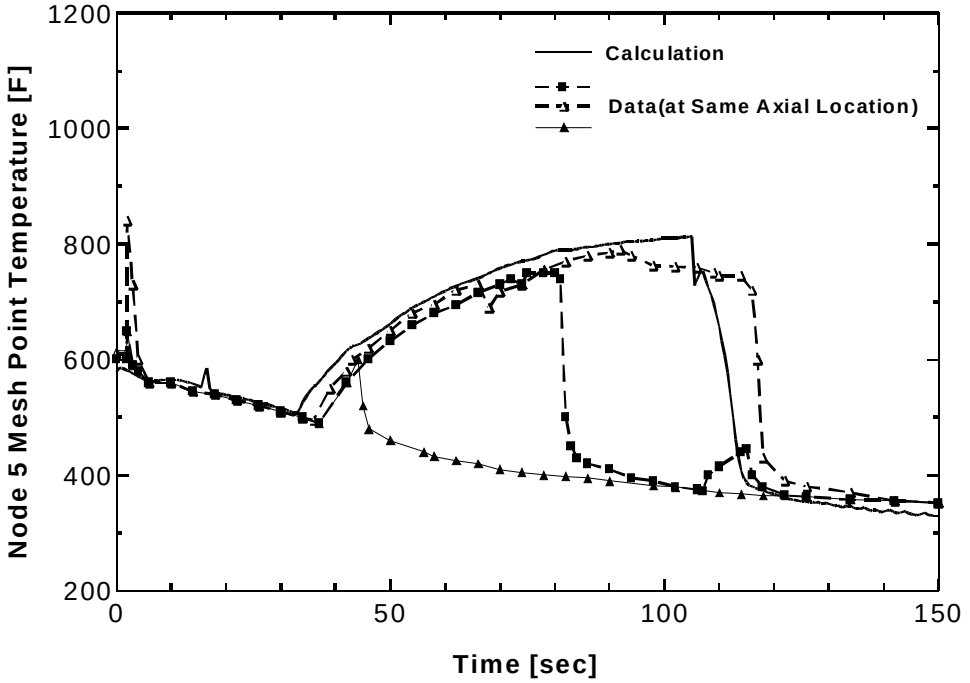

Fig.15(b) Cladding temperature comparison at node 5 for the TLTA-5A/6424 RUN1

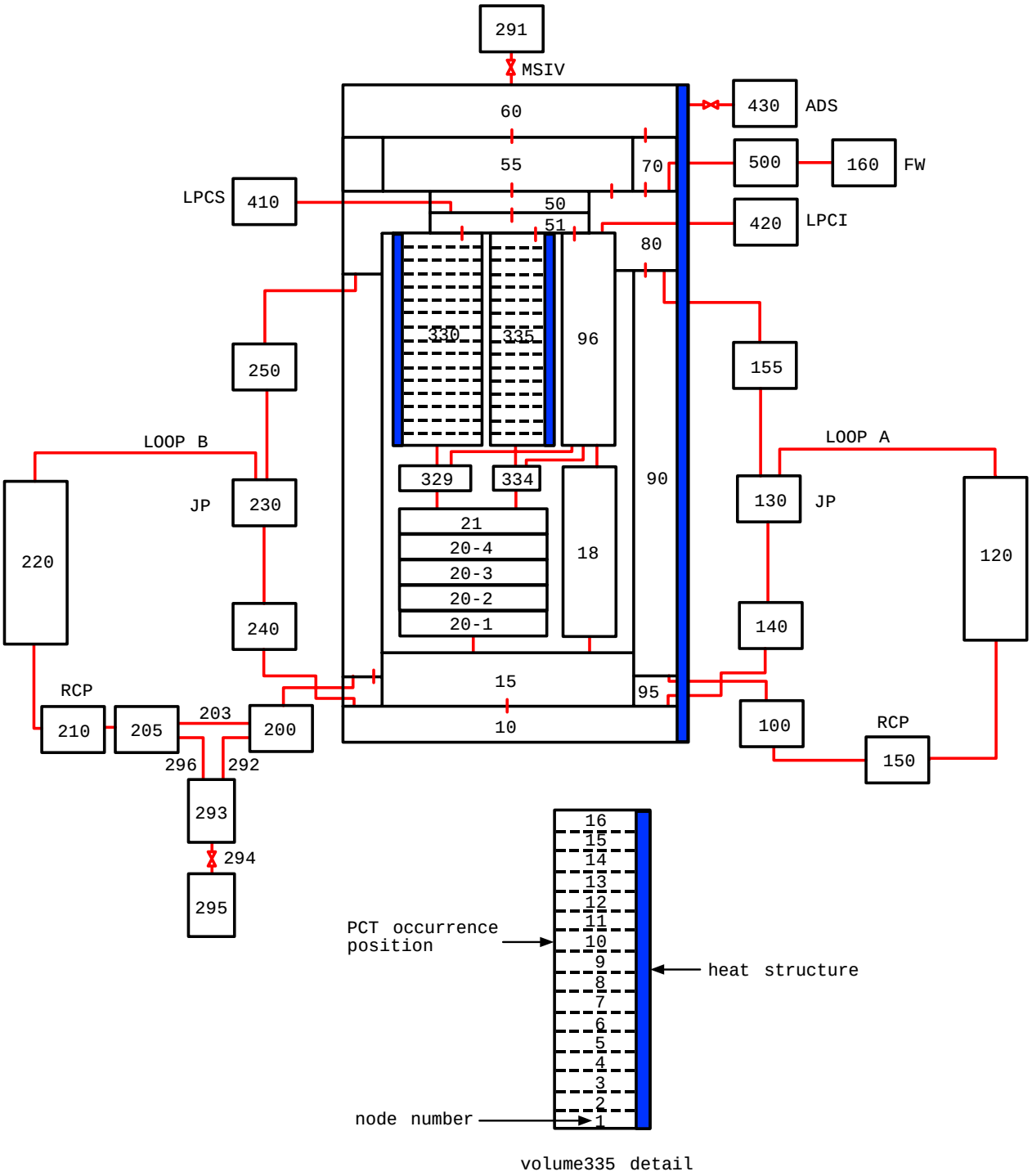

Fig.16 Analysis model for the ROSA-III RUN912

Table 3 Calculation cases for the ROSA-III Run 912

Case	Description
1	Kataoka-Ishii interface friction without two-phase mixture level model
2	Kataoka-Ishii interface friction with two-phase mixture level model (Donor cell)
3	Original interface friction without two-phase mixture level model
4	Case2 + One lower plenum node[*1] with no guide tube
5	Case2 + Two upper plenum node[*2]

*1 The node includes the original nodes of 15,20,21,329 and 334 in Fig.16

*2 The node 15 in Fig.16 is divided into 2 nodes

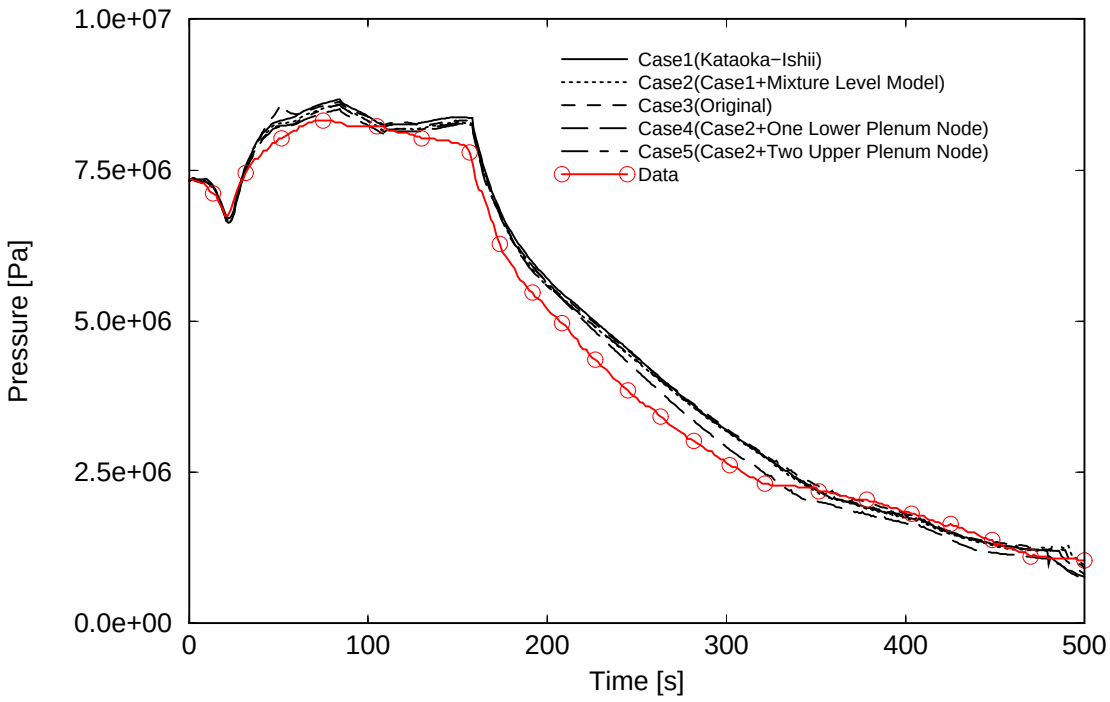

Fig.17 Pressure comparison fort the ROSA-III RUN 912

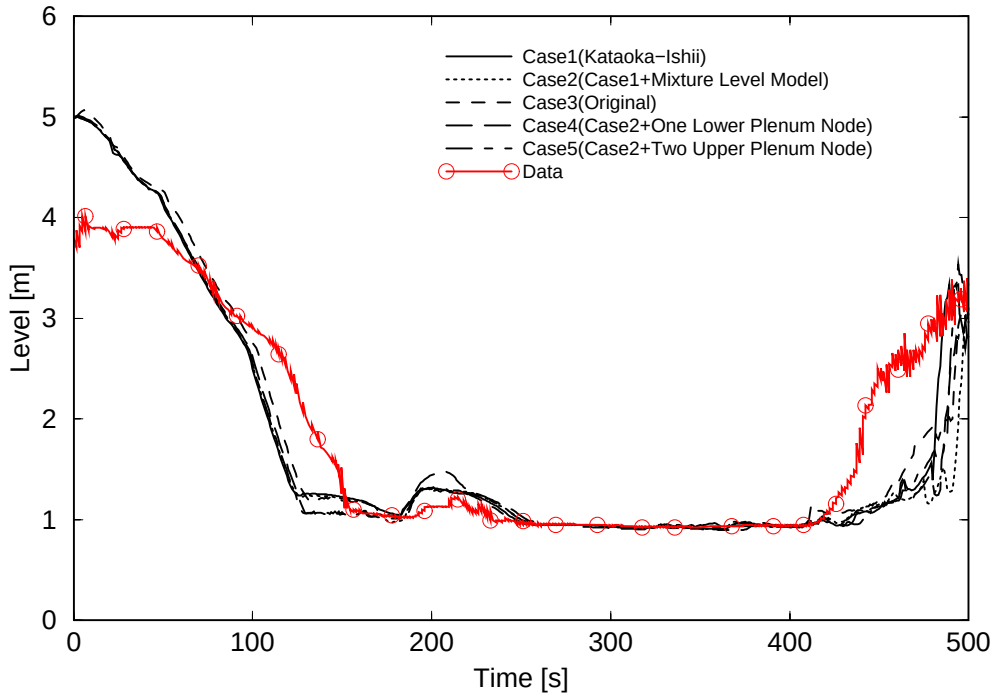

Fig.18 Downcomer collapsed water level comparison fort the ROSA-III RUN 912

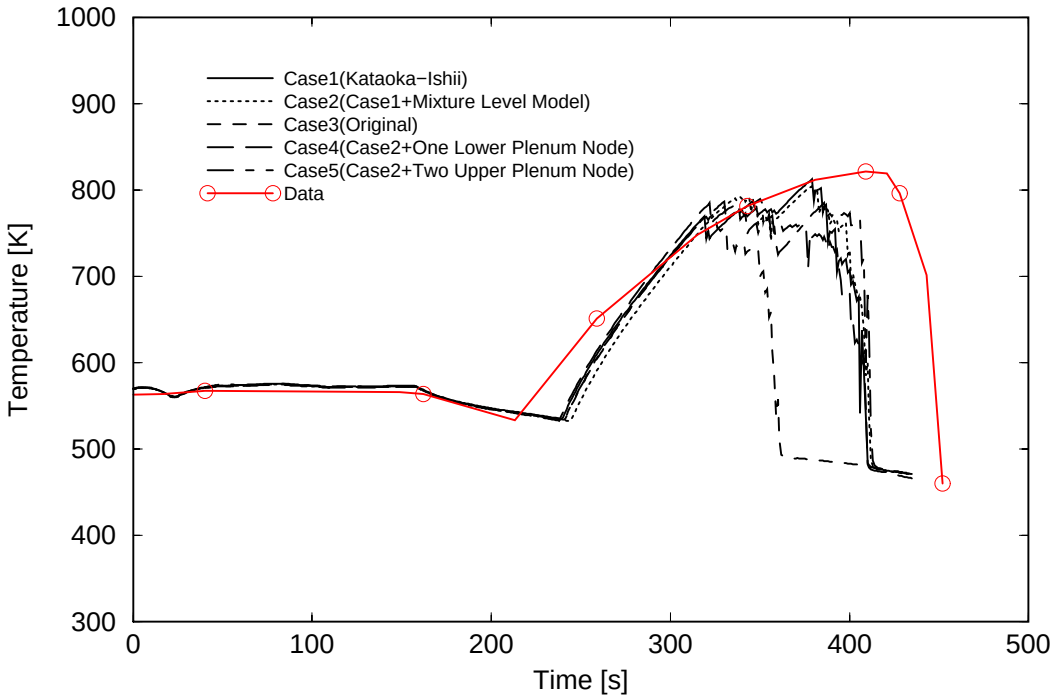

Fig.19 Peak cladding temperature comparison fort the ROSA-III RUN 912

4. DATA QUALIFICATION FOR LOCA ANALYSIS

From the experiences of sensitivity analyses, the original CHF and post-dryout heat transfer correlation give more conservative results in comparison with the incorporated models in the blowdown phase. In the reflood phase the CCFL model is indispensable to properly simulate the experimental trend. The choice of interfacial friction, rewetting, and by-pass leak flow models have a large influence on PCT. The effect of such models as CCFL breakdown, spray water behavior (UPM) is not so clear in the analyses of integral tests. This might be due to the rather small diameter of the upper plenum in the integral tests analyzed. It can be said that these models should be used in the actual plant analysis. These considerations and findings from experimental analyses are reflected to the standard input data for the actual plant analysis. The list of standard option is shown in Table 4.

Table 4 Standard option in the input data for actual 1100MWe BWR plant analysis

Item	Standard option
Boiling Transition	CPR based prediction model
Post dryout heat transfer during blowdown	Groenveld heat transfer coefficient + liquid droplet cooling
Rewet during blowdown	CPR based rewet model (MCPR >1 + Iloeje model)
Interface friction	EPRI model in the fuel bundle Kataoka-Ishii model in the other components
CCFL	SEO (Kutateladze type) Upper tie-plate (Kutateladze type)
CCFL breakdown	Not used
Spray water behavior	Upper plenum is divided into multi-volume (UPM)
By-pass leak flow	Form loss coefficient
Rewet during reflood	Groenveld heat transfer coefficient + liquid droplet cooling
Discharge coefficient	0.825

5. CONCLUSION

Modifications were performed for such models in the RELAP5/MOD2 as the prediction of boiling transition, post-dryout heat transfer, interfacial friction, counter-current flow limiting (CCFL), CCFL breakdown, rewetting at reflood phase, the spray water behavior, and the two-phase mixture level; and they have been qualified against separate effect test data. The TLTA and the ROSA-III experiments were used to verify the integral performance of the code and the code was named RELAP5/MOD2/INS.

With these wide ranges of model modifications and validation efforts, the original RELAP5/MOD2 code is enhanced to be the RELAP5/MOD2/INS code; the Best Estimate analysis tool for LOCA audit analyses for Boiling Water Reactors. Though there still exist some non-conservative results in the analysis of integral tests, the code is adequate on a BE basis. Some of the parameters and physical models sensitive to the BWR LOCA phenomena have been identified and reflected in the standard input data for actual plant analysis. At the same time, the conformance of the physical models to the "ECCS Performance Evaluation Guide" was confirmed. At present, we are investigating a methodology of the uncertainty evaluation and its effective usage. Therefore, conservative analytical conditions and model parameters will be used for audit analyses for the time being.

NOMENCLATURE

C	constant in CCFL correlation
G	mass flux
h	heat transfer coefficient
K	non-dimensional mass flux
m	constant in CCFL correlation
q	heat flux
S	Chen’s boiling suppression factor
t	time
T	temperature
Δ	difference
ε	constant in Weisman transition boiling heat transfer coefficient

Subscripts

cr	critical
f	fluid
g	gas
m	mean
min	minimum
ref	reference
sat	saturation
w	wall

ACKNOWLEDGMENTS

This work was performed under the sponsorship of the Ministry of International Trade and Industry.

REFERENCES

Analytis, G. and Richner, G., 1987. Effect of Bubbly/Slug Interfacial Shear on Liquid Carryover Predicted by RELAP5/MOD2 During Reflooding, Transactions American Nuclear Society, 53 pp. 540-41.

Anklam, T.M., et al. Experimental Investigation of Uncovered-Bundle Heat Transfer and Two-phase Level Swell under High Pressure Low Heat Flux Conditions, NUREG/CR-2456, March 1982.

BWR Refill-Reflood Program Task 4.4–30 SSTF Description Document, NUREG/CR-2133, May 1982.

Bankoff, S.G., et.al., 1981. Countercurrent Flow of Air/Water and Steam/Water Through a Horizontal Perforated Plate, Int. J. Heat Mass Transfer, Vol.24, No.8, 1381-1395.

Chexal, B. and Lellouche, G., 1986. A full-Range Drift-Flux Correlation for Vertical Flows (Revision 1), EPRI NP-3989-SR, (Sept. 1986)

Collier, J.G. 1972. Convection Boiling and Condensation, London: McGraw-Hill Book Company, Inc

Dongarra, J.J., Moler, C.B., Bunch, J.R. and Stewart, G.W. 1979. LINPACK User's Guide SIAM, Philadelphia.

Dukler, A.E. and Smith, L., Two-Phase Interactions in Countercurrent Flow: Studies of Flodding Mechanism, NUREG/CR-0617, 1979.

Groeneveld, D.C.,1973. Post Dryout Heat Transfer at Operating Conditions, Proc.Tech.Mtg.on Water Reactor Safety, CONF-73030K, U.S.Atomic Energy Commission.

Grutter, F. et al., NEPTUN Bundle Reflooding Experiments: Test Facility Description, EIR-Report No. 386, 1981.

Hassan, Y., 1986. Analysis of FLECHT Reflood Tests woth RELAP5/MOD2, Nuclear Technology, Vol.74 August, pp.176-188.

Iloeje, et. al., O.C., 1995. An Investigation of the Collapse and Surface Rewet in Film Boiling in Forced Vertical Flow, Trans.ASME J. of Heat Transfer.

Jones, D.D., Subcooled Countercurrent Flow Limiting Characteristics of the Upper Region of a BWR Fuel Bundle, NEDG-NUREG-23549, 1977.

Kasahara, F et.al., 1977. Recent Modeling Improvements of RELAP5/MOD2 for LOCA Analysis at NUPEC, 11th CAMP meeting OCT. 22-23, Bethesda, Maryland

Kasahara,F et al., 1998. Modification of RELAP5/MOD2 Code and its Application for BWR LOCA Analysis, 12th CAMP meeting JUN. 22-23, Ankara, Turkey

Kataoka, I. and ISHII, M., 1987. Drift Flux Model for Large Diameter Pipe and New Correlation for Pool Void Fraction, International Journal of Heat and Mass Transfer, 30, pp. 1927-39.

Kitamura,M. et al.,1998. BWR 9x9 type Fuel Assembly Critical Power Test at High-Pressure Conditions, ICONE-6410, May.

Kutateladze, S.S., 1972. Elements of Hydrodynamics of Gas-Liquid Systems, Fluid Mechanics – Soviet Resarch, Vol.1, pp. 29-50.

Lee, L.S. et al. BWR Large Break Simulation Tests BWR Blowdown/Emergency Core Cooling Program, Vol. 1., Vol.2, NUREG/CR-2229, April 1982.

Mitsutake, T. et al.,1997. Study on Rod Surface Temperature Behavior of BWR 8x8 High Burn-up Fuel Assembly under Post Boiling Transition Condition, NUREH-8, Proceedings Volume 3

Murase, M and Susuki,H., 1985 Evaluation of Countercurrent Gas/Liquid Flow in Parallel Channels with Restricted Ends. Nucl. Technol., 68, 408.

Nagasaka, H. et al, 1984. BWR Core Cooling in Refill/Reflood Phase, 12th LWR Safety Research Information Meeting, Gaithersburg, Maryland.

Nagasaka, H. et al. 18 Degree Sector System Test (ESTA-II), NUREG/CP-0058,Vol.3 ,1984.

Nagasaka, H. et al., 1985. New Japanese Correlation on Core Cooling and CCFL Characteristics during BWR LOCA, 13th LWR Safety Research Information Meeting, Gaithersburg, Maryland.

Nakamura, H., et al. ROSA-III 200% Double-ended Break Integral Test Run 926(HPCS Failure), JAERI-M 84-008, February 1984

Sun,K.H., 1979. Flooding Correlation for BWR Bundle Upper Tie-plates and Bottom Side-Entry Orifices, Second Multi Phase Flow and Heat Transfer Symposium-Workshop, Miami Beach, FL, April 16-19.

Wallis, G.B. et al., Countercurrent Annular Flow Regimes for Steam and Subcooled Water in a Vertical Tube, EPRI, NP-1336, January 1980.

Weisman, J. Studies of Transition Boiling Heat Transfer at Pressure from 1-4 Bar, EPRI Report NP-1899, 1981

Zuber, N. and Findlay, J.,1965. Average Volumetric Concentrations in Two-Phase Flow Systems, Journal of Heat Transfer, **87**, pp.453-586.